SAND2015-2986C

Exceptional service in the national interest

Sandia National Laboratories

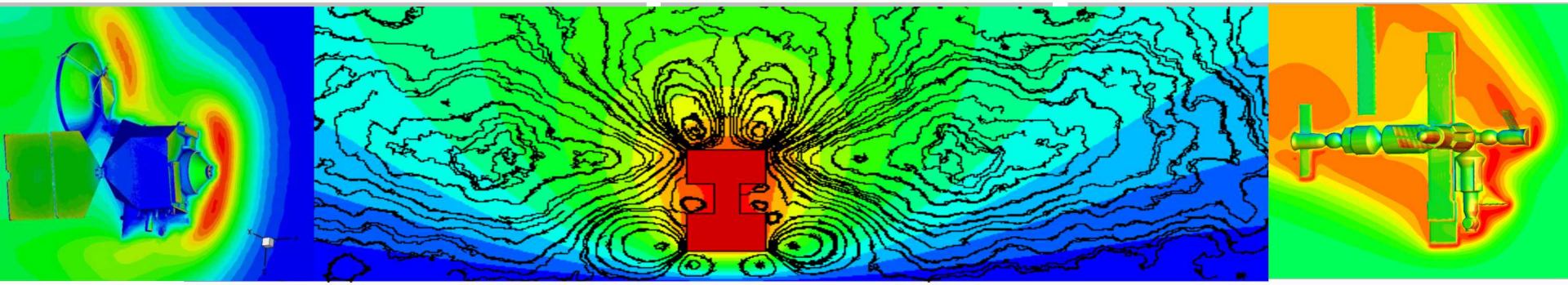

Molecular-Level Simulations of Hydrodynamic Instabilities in Gases

Michael A. Gallis

Engineering Sciences Center
Sandia National Laboratories
Albuquerque, New Mexico, USA

U.S. DEPARTMENT OF ENERGY

NNSA National Nuclear Security Administration

Sandia National Laboratories is a multi-program laboratory managed and operated by Sandia Corporation, a wholly owned subsidiary of Lockheed Martin Corporation, for the U.S. Department of Energy's National Nuclear Security Administration under contract DE-AC04-94AL85000.

Collaborators

Sandia National Laboratories


John Torczynski


Dan Rader


Tim Koehler


Steve Plimpton

The Columbia Accident

Sandia National Laboratories

On February 1st 2003 STS-107 with Shuttle orbiter Columbia disintegrated over western Texas, minutes before it was scheduled to land.

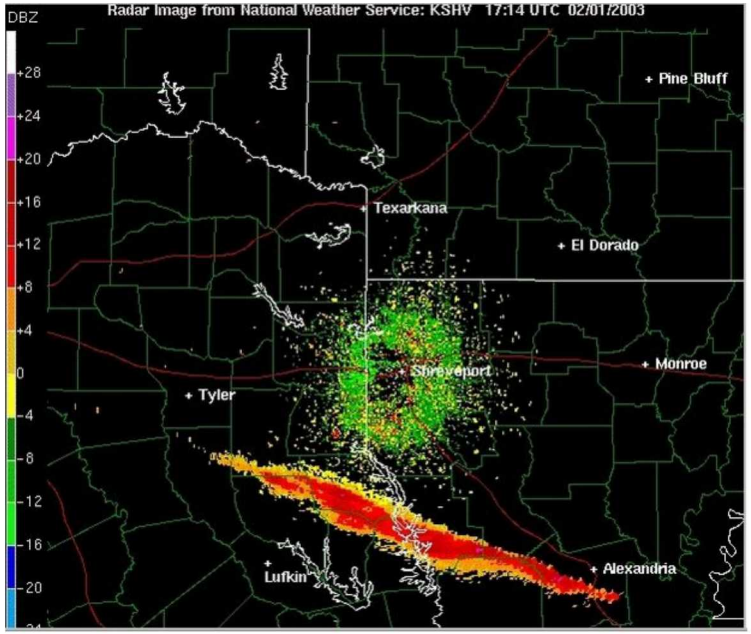

Foam impact during launch

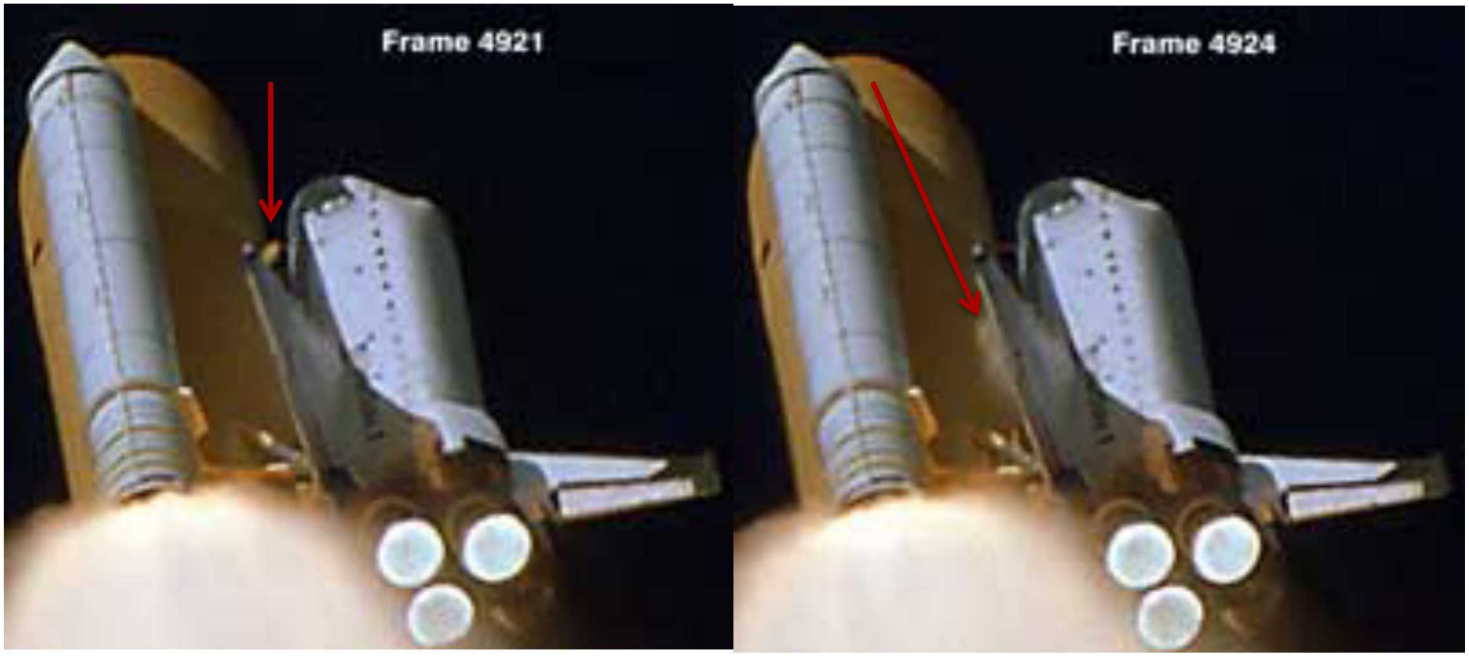

During the ascent phase a piece of foam insulation broke off from the shuttle's propellant tank damaging (?) the shuttle's left wing.

Damage Scenario Investigated

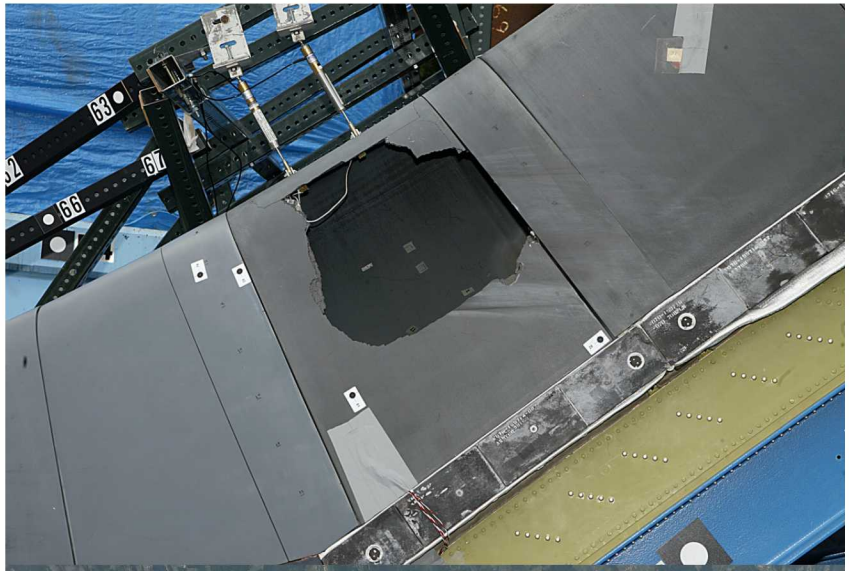

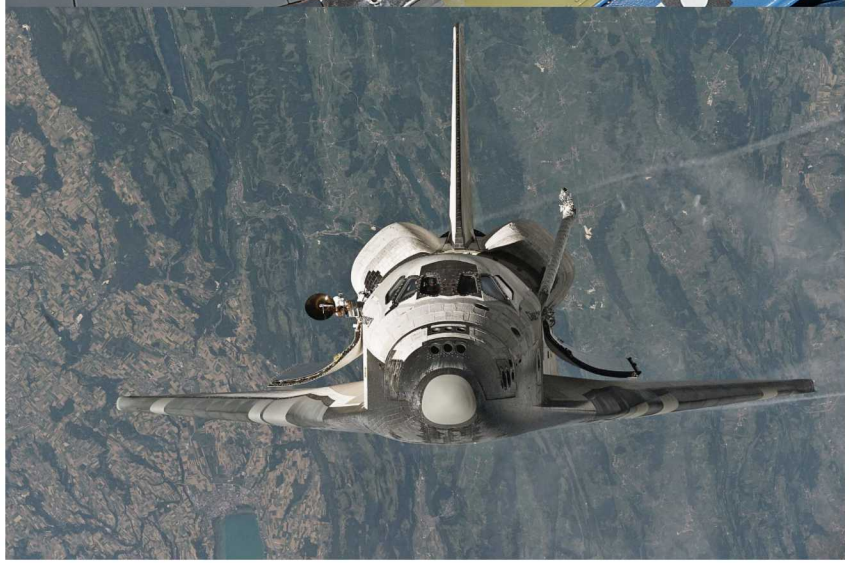

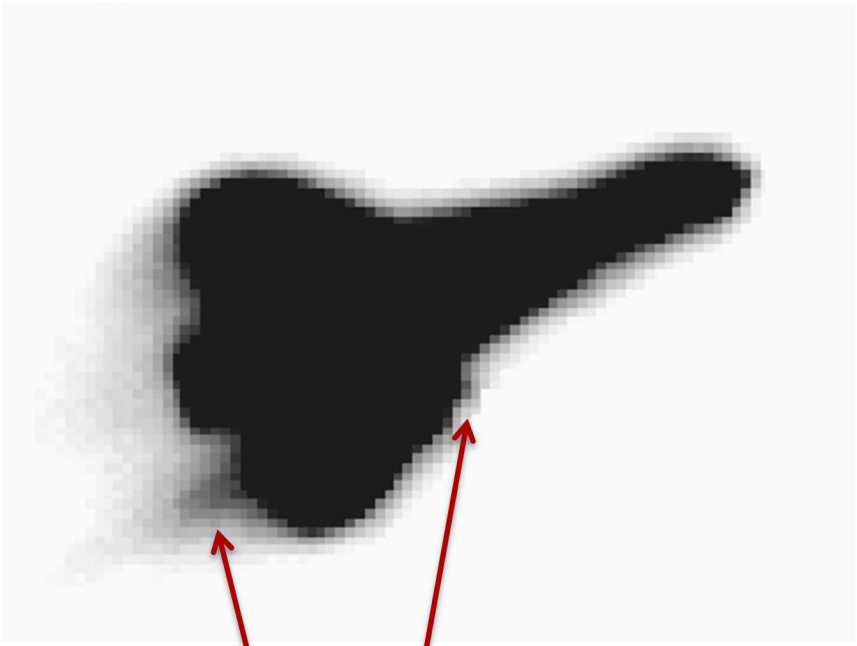

The resulting hole allowed overheated gases to burn through the wing cavity, compromise its structural integrity, leading to a loss of the vehicle during descent

Numerical Simulations Supporting the Investigation

Sandia National Laboratories

Simulation conditions

Altitude = 350,000-300,000 ft

Mach Number = 27

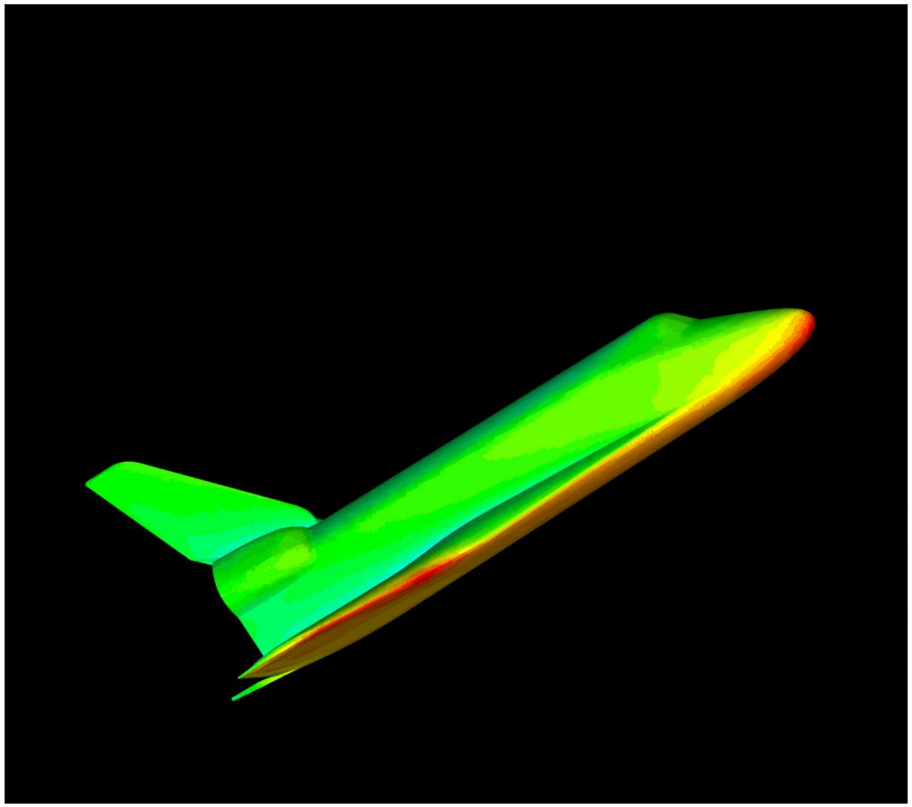

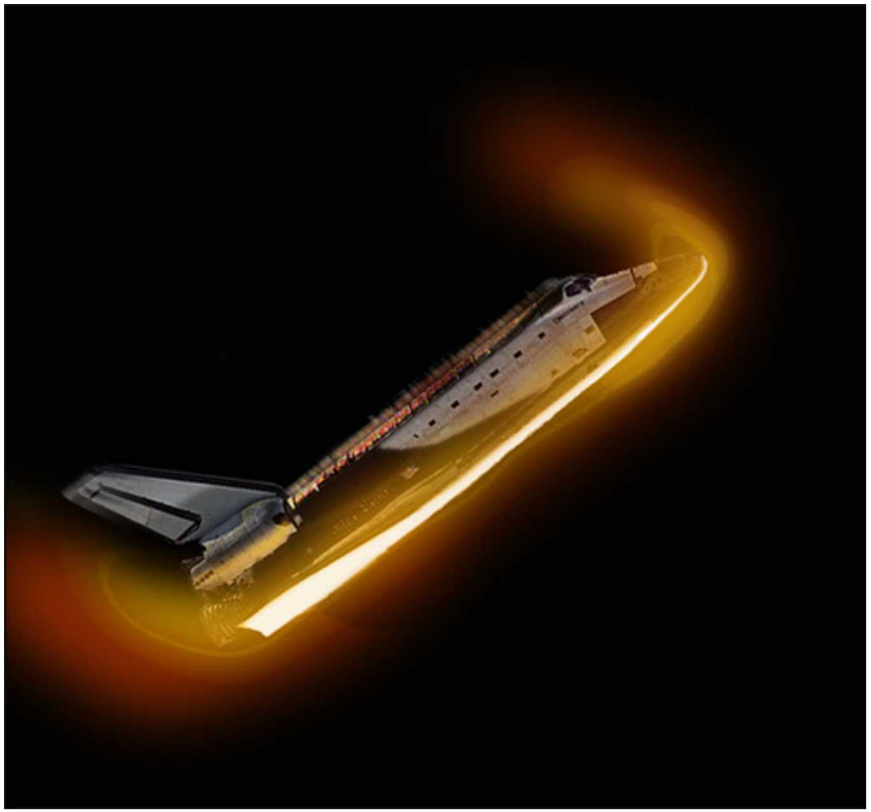

Temperature and Heating Profile

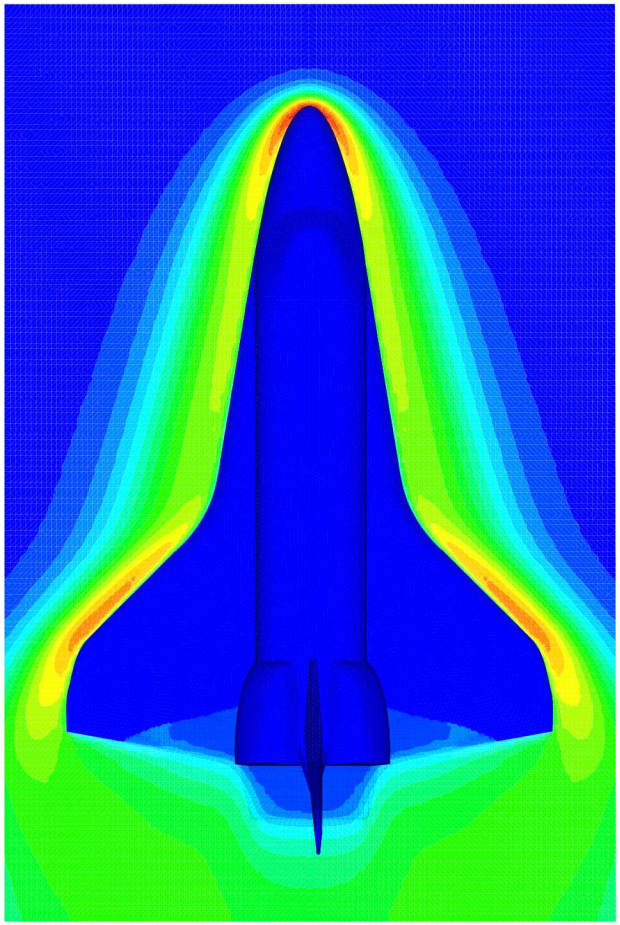

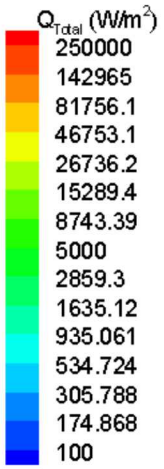

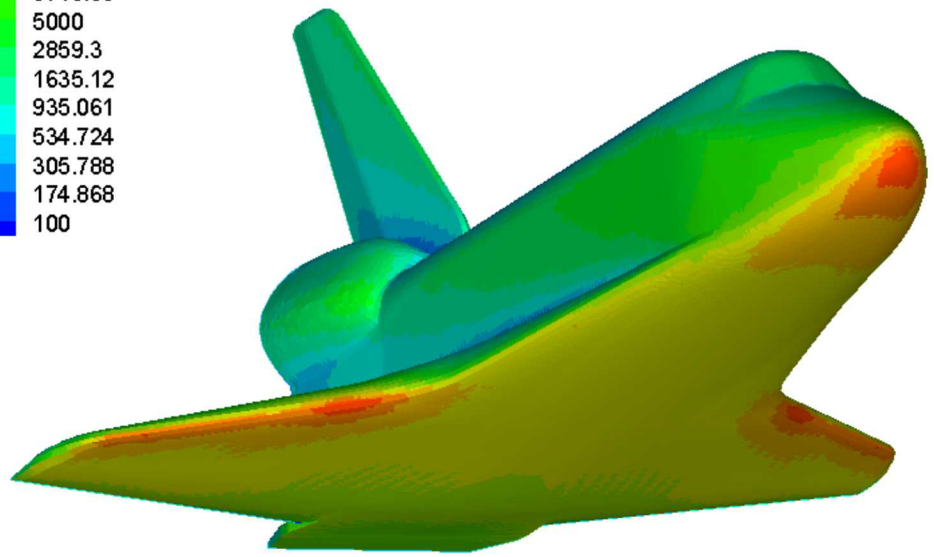

Flow Inside the Wing Cavity

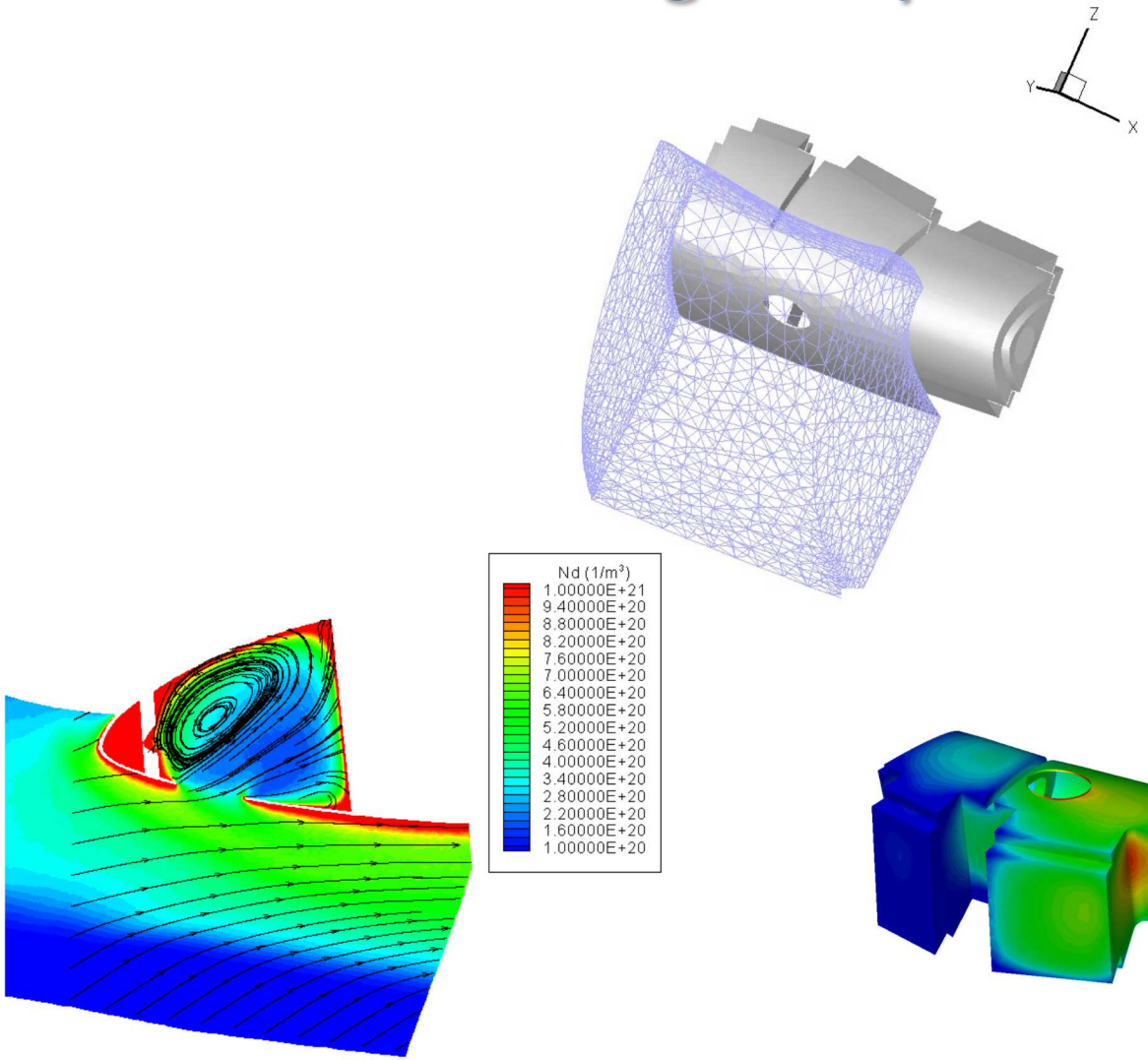

The Mars Reconnaissance Orbiter mission

- Launch Date : August 12 2005
- Mars Orbit insertion : March 10 2006
- Final Orbit reached : August 30 2006

Scope of MRO DSMC analysis

Sandia National Laboratories

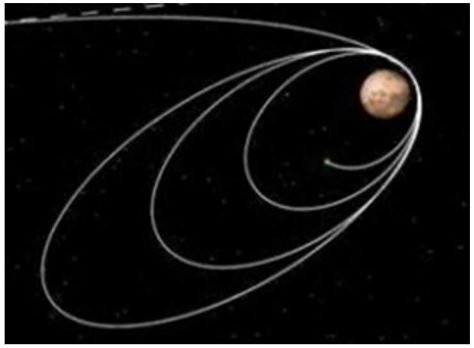

- Aerobraking was used to reduce fuel requirements during orbit placing maneuvers
- From a highly elliptic orbit the spacecraft was brought down to a near circular science orbit (255-320 km)
- During the maneuvers the vehicle had to be aerodynamically stable and the heat load could not exceed maximum values

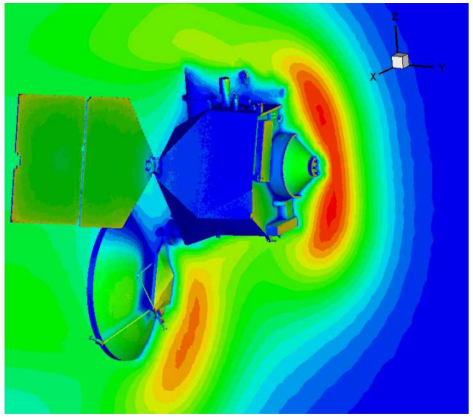

Scope of the following calculations:

- Determine the heat transfer to the vehicle for a number of angles of attack at nominal aerobraking altitude and velocity
- Determine drag for a number of altitudes

Heat flux for nominal aerobraking conditions

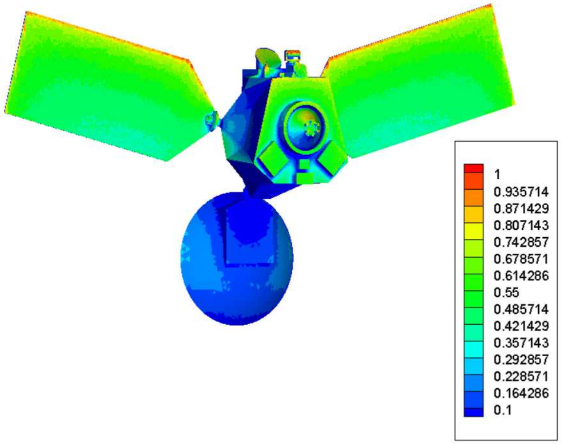

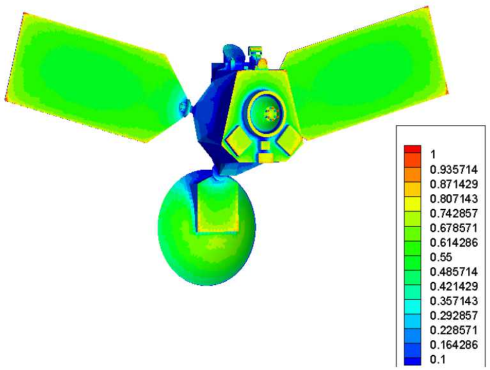

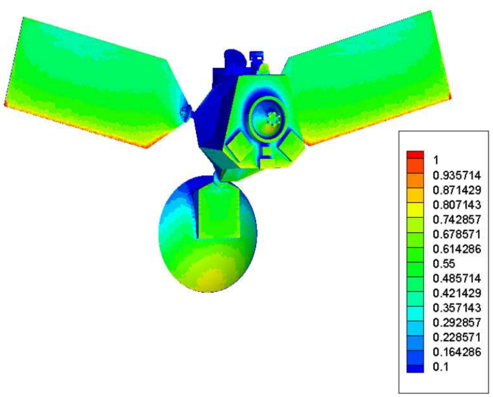

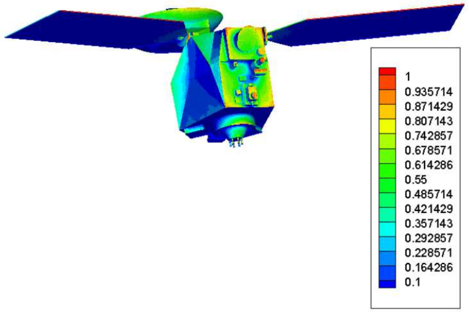

Length Scales for Dilute Gases

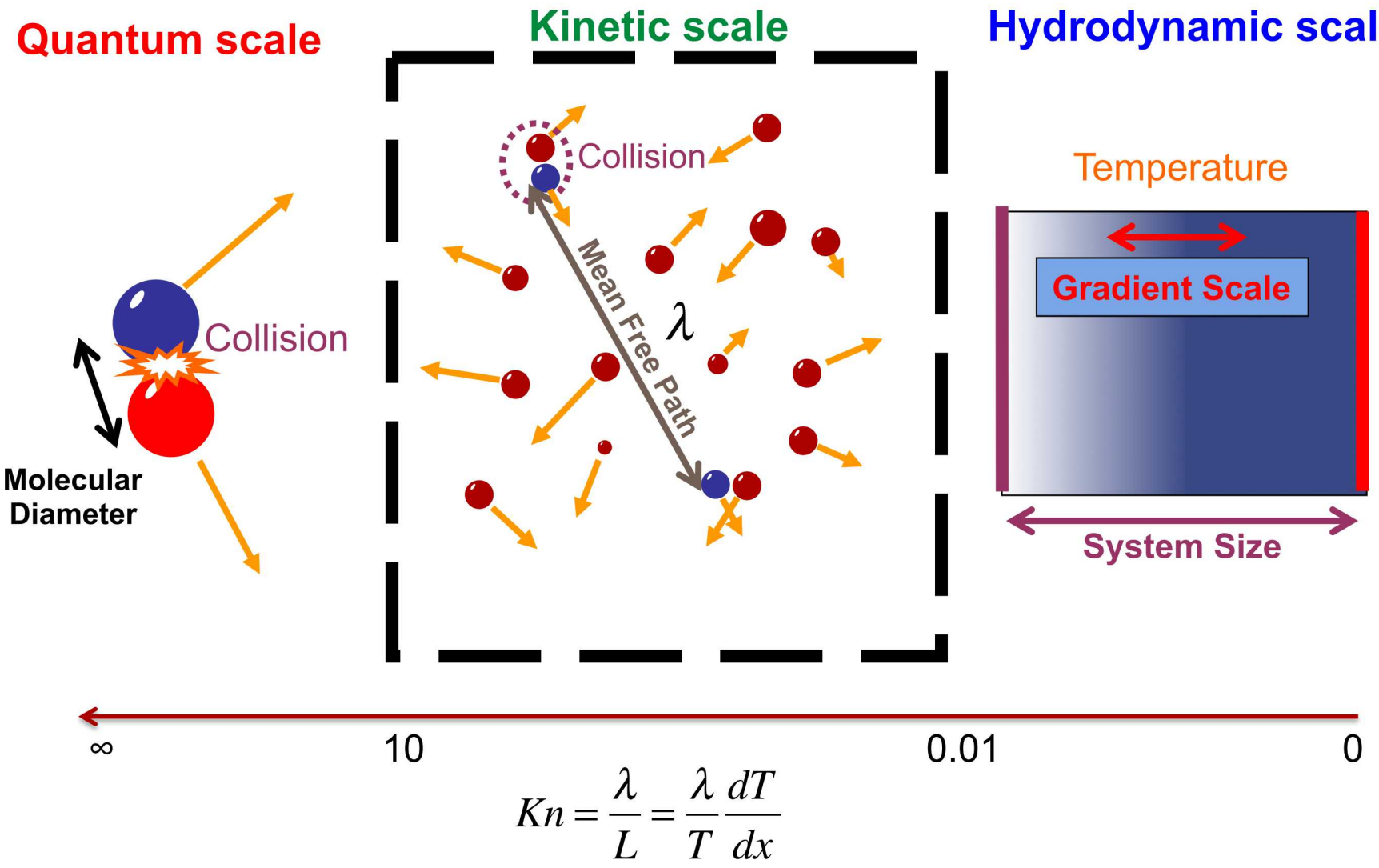

$$Kn = \frac{\lambda}{L} = \frac{\lambda}{T}\frac{dT}{dx}$$

Non-equilibrium effects

Sandia National Laboratories

Non-equilibrium effects:

- Non-Maxwell, Chapman-Enskog velocity distribution functions
- Non-linear transport properties
- Non-Boltzmann internal energy, no energy equipartition
- Non-Arrhenius chemical reactions
- Non-continuous temperature and velocity profiles (Knudsen layers close to walls)

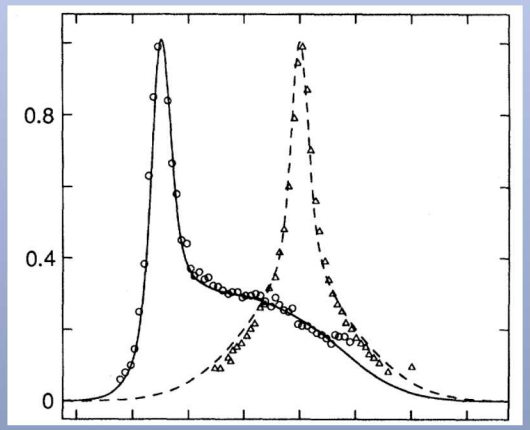

Non-equilibrium velocity distribution functions in the front a Mach 25 normal shock of helium
Pham-Van-Diep, *et al.* , *Science*, 1989

- Can be caused by:
  - Reduced collisionality (low density)
  - Strong gradients even in near-continuum conditions

Boltzmann Equation and the Direct Simulation Monte Carlo Method (DSMC)

Sandia National Laboratories

Ludwig Boltzmann

$$\frac{\partial f}{\partial t} + \mathbf{v}\cdot\frac{\partial f}{\partial \mathbf{x}} + \frac{\mathbf{F}}{m}\cdot\frac{\partial f}{\partial \mathbf{v}} = \int_{-\infty}^{\infty}\int_{0}^{4\pi}\left(f^{*}f_{1}^{*} - ff_{1}\right)\left|\mathbf{v}-\mathbf{v}_{1}\right|\sigma\, d\Omega\, d\mathbf{v}_{1}$$

molecular motion and force-induced acceleration

pairwise molecular collisions (molecular chaos)

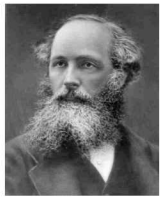

James Clerk Maxwell

$f(\mathbf{r},\mathbf{c},t)d^3rd^3c \rightarrow$ Expected number of molecules at time t in at $\mathbf{r}+d^3r,\mathbf{c}+d^3c$

$$n(\mathbf{r},t) = \int f(\mathbf{r},\mathbf{c},t)d^3c$$

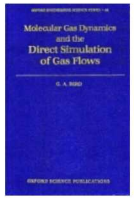

Graeme Bird (1963, 1994)

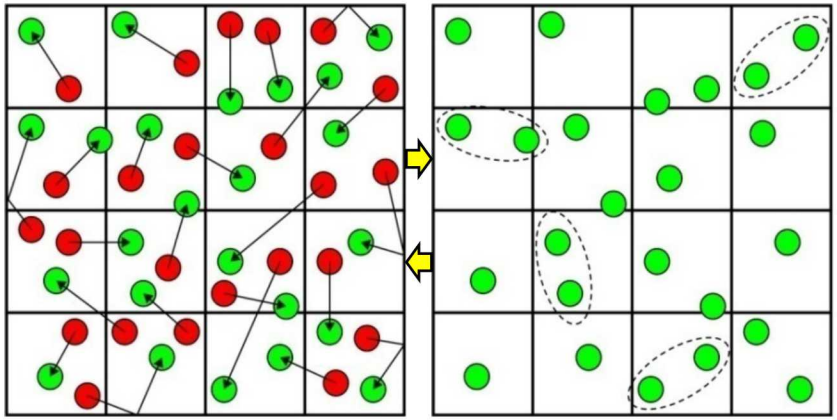

molecules move

molecules collide

DSMC is a physical, statistical, molecular-level simulation method

Simulating the Kinetic Regime

H. W. Liepmann

A. Roshko

G. A. Bird

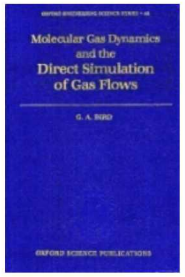

- "In general, the field or rarefied gas flow problems is still largely unclarified" last sentence from *Elements of Gasdynamics (1956)* by Hans W. Liepmann and Anatol Roshko.
- The Direct Simulation Monte Carlo (DSMC) originated in 1963 by Graeme A. Bird, encouraged by Hans W. Liepmann.
  * "G. A. Bird, 'Approach to translational equilibrium in a rigid sphere gas', Phys. Fluids, 6, p1518 (1963)".
- The objective of DSMC is to simulate complicated gas flows using only collision mechanics of simulated molecules
- Today, DSMC is the dominant numerical algorithm at the kinetic scale
- DSMC applications are expanding to multi-scale problems creating new challenges and opportunities.

Direct Simulation Monte Carlo

Sandia National Laboratories

How DSMC works

DSMC molecule-simulators **statistically** represent a large number of real molecules ($O(10^{10})$-$O(10^{15})$)

Computational molecules move ballistically, collide statistically, and interact statistically with surfaces **like real molecules**

Molecular movement, surface-interaction, and collision are implemented **sequentially** in the algorithm

Cell-based molecular statistics ("moments") are sampled and averaged over many time steps for steady flow

DSMC is inherently a transient method

Steady state is the ensemble average of unsteady state moves

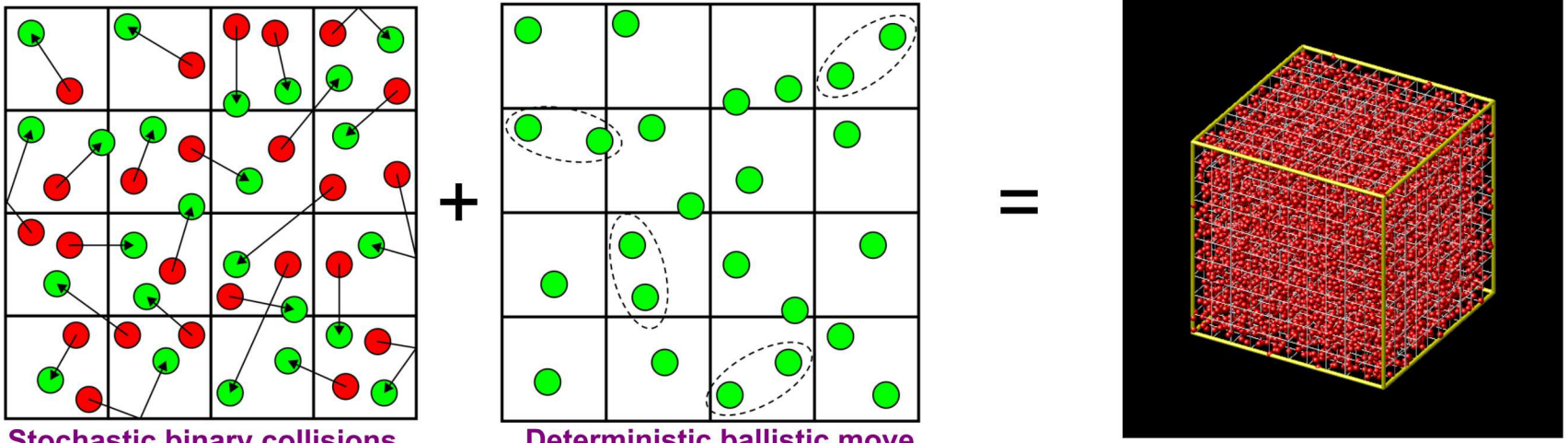

Stochastic binary collisions

Deterministic ballistic move

DSMC vs. Boltzmann Equation

Sandia National Laboratories

- Instead of solving Newton's laws of motion (Molecular Dynamics), DSMC replaces explicit intermolecular forces with stochastic collisions
- It has been shown that DSMC is equivalent to solving the Boltzmann equation (Nambu 1980, Babovsky 1989, Wagner 1992)
- DSMC has been shown to reproduce exact known solutions (Chapman-Enskog, Moment Hierarchy) of the Boltzmann equation (Gallis et al. 2004, 2006) for non-equilibrium flows
- In fact, DSMC is superior to solving the Boltzmann equation
  - DSMC can model complicated processes (e.g., polyatomic molecules, chemically reacting flows, ionized flows) for which Boltzmann-type transport equations are not even known (Struchtrup 2005)
  - DSMC includes fluctuations, which have been shown to be physically realistic (Garcia 1990) but which are absent from the Boltzmann equation

The objective of DSMC is to simulate complicated gas flows using only collision mechanics of simulated molecules in the regime described by the Boltzmann equation

Navier-Stokes vs. Boltzmann Equation

Sandia National Laboratories

- The Navier-Stokes equations for gases can be derived from the Boltzmann equation assuming:
  - Near-equilibrium conditions
  - Local Thermodynamic Equilibrium (LTE)
  - Continuum medium
- Conservations equations (mass, momentum, energy) can be derived as averages of molecular properties
- Transport is given by averaging molecular fluxes. Under LTE Newton's, Fourier's and Fick's laws are obtained

George Stokes

Claude Navier

Quantifying Non-Equilibrium
Fourier and Couette Flow

Sandia National Laboratories

Joseph Fourier

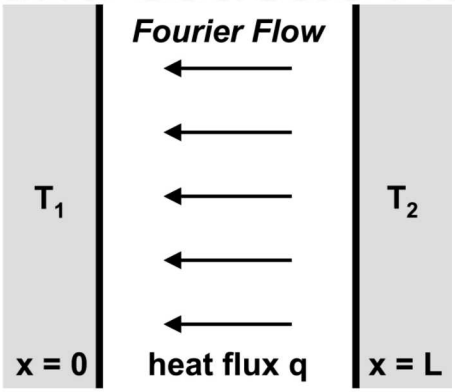

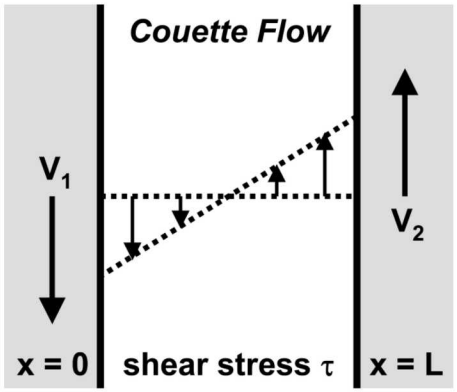

Maurice Couette

$$q = -K\frac{\partial T}{\partial x}$$

$$\tau = \mu\frac{\partial v}{\partial x}$$

Investigate transport in gas between parallel plates

- Fourier flow: heat conduction in stationary gas
- Couette flow: momentum transport in isothermal shear flow

Apply DSMC to Fourier flow and Couette flow

- Heat flux, shear stress: one-dimensional, steady

Compare DSMC to analytical "normal solutions"

- Normal: outside Knudsen layers
- Solutions: Chapman-Enskog (CE), Moment-Hierarchy (MH)

Verify DSMC accuracy at arbitrary heat flux, shear stress

- Thermal conductivity, viscosity; velocity distribution

Near-Equilibrium: Chapman-Enskog (CE) Theory

Sydney Chapman

David Enskog

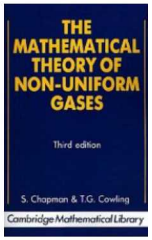

$$f = f^{(0)}(1+\Phi^{(1)}+\Psi^{(1)}) \qquad f^{(0)} = (n/\pi^{3/2}c_m^3)\exp[-\tilde{c}^2]$$

$$c_m = \sqrt{2k_BT/m} \qquad \tilde{\mathbf{c}} = \mathbf{c}/c_m \quad \mathbf{c} = \mathbf{v}-\mathbf{u}$$

$$\Phi^{(1)} = -(8/5)\tilde{A}[\tilde{c}]\tilde{\mathbf{c}}\cdot\tilde{\mathbf{q}} \qquad \Psi^{(1)} = -2\tilde{B}[\tilde{c}](\tilde{\mathbf{c}}\circ\tilde{\mathbf{c}}:\tilde{\tau})$$

$$K = -(5/4)k_Bc_m^2a_1 \qquad \mu = (1/2)mc_m^2b_1$$

$$\tilde{A}[\tilde{c}] = \sum_{k=1}^{\infty}(a_k/a_1)S_{3/2}^{(k)}[\tilde{c}^2] \qquad \tilde{B}[\tilde{c}] = \sum_{k=1}^{\infty}(b_k/b_1)S_{5/2}^{(k-1)}[\tilde{c}^2]$$

$$C_p = (5/2)(k_B/m) \qquad \mathrm{Pr} = (2/3)(\mu_\infty/\mu_1)(K_1/K_\infty)$$

- Chapman and Enskog analyzed Boltzmann collision term
  - Perturbation expansion using Sonine polynomials
  - Near equilibrium, appropriate in continuum limit
- Determined velocity distribution and transport properties
  - Thermal conductivity K, viscosity μ, mass self-diffusivity D
  - Prandtl number Pr from "infinite-to-first" ratios K_∞/K_1, μ_∞/μ_1
  - Distribution "shape": Sonine polynomial coeffs. a_k/a_1, b_k/b_1
  - Values for all Inverse-Power-Law (IPL) interactions
    - Maxwell and hard-sphere are special cases

Extracting CE Parameters from DSMC

Sandia National Laboratories

$$q = K_{eff}\left(\frac{\partial T}{\partial x}\right) \qquad \frac{a_k}{a_1} = \sum_{i=1}^{k}\left(\frac{(-1)^{i-1}k!(5/2)!}{(k-i)!i!(i+(3/2))!}\right)\left(\frac{\left\langle \tilde{c}^{2i}\tilde{c}_x\right\rangle}{\left\langle \tilde{c}^{2}\tilde{c}_x\right\rangle}\right) \qquad \tilde{\mathbf{c}} = \frac{\mathbf{v}-\mathbf{V}}{c_m}$$

$$\tau = \mu_{eff}\left(\frac{\partial V}{\partial x}\right) \qquad \frac{b_k}{b_1} = \sum_{i=1}^{k}\left(\frac{(-1)^{i-1}(k-1)!(5/2)!}{(k-i)!(i-1)!(i+(3/2))!}\right)\left(\frac{\left\langle \tilde{c}^{2(i-1)}\tilde{c}_x\tilde{c}_y\right\rangle}{\left\langle \tilde{c}_x\tilde{c}_y\right\rangle}\right) \qquad c_m = \sqrt{\frac{2k_BT}{m}}$$

DSMC moments of velocity distribution function

- Temperature T, velocity V
- Heat flux q, shear stress τ
- Higher-order moments

DSMC values for VSS molecules (variable-soft-sphere)

- Thermal conductivity and viscosity: K_{eff} and μ_{eff}
- Sonine-polynomial coefficients: a_k/a_1 and b_k/b_1
- Applicable for arbitrary Kn_L, Kn_q, Kn_τ

Temperature and Velocity Profiles

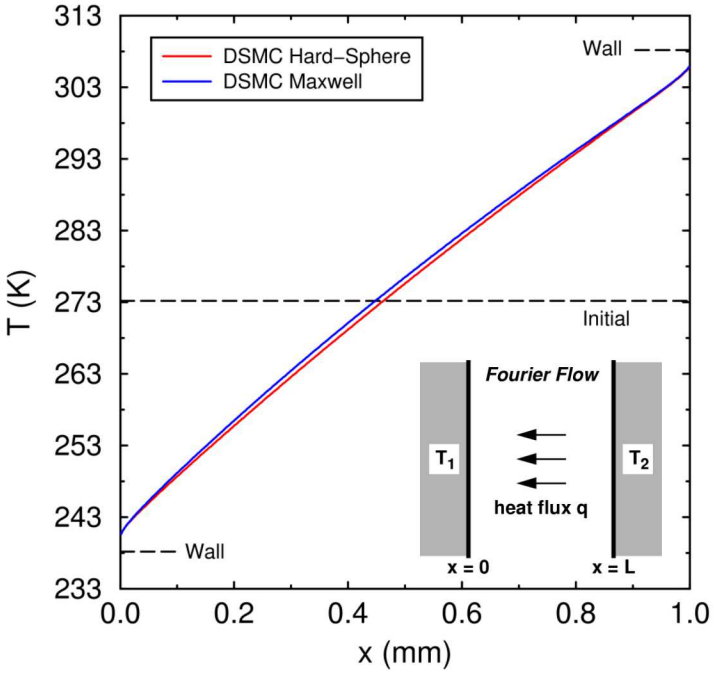

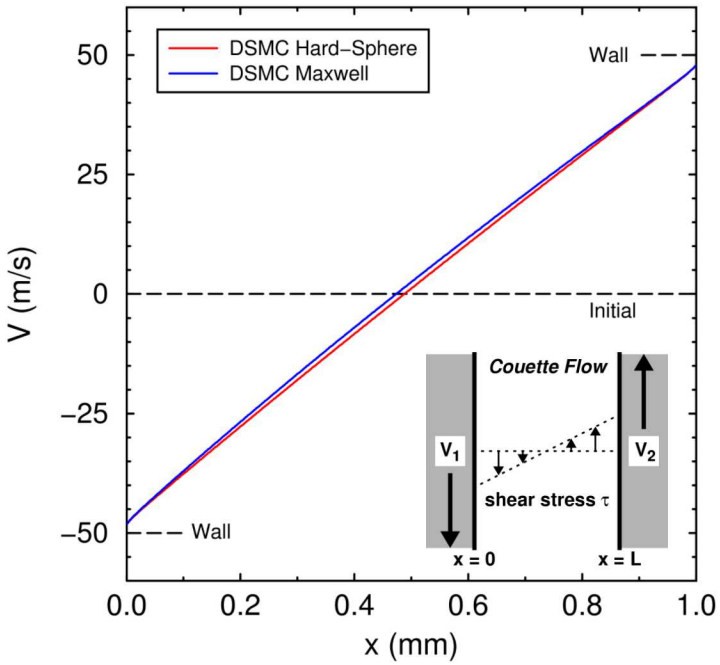

Low heat flux and shear stress: $Kn_q = 0.006$, $Kn_\tau = 0.003$

- Argon-like: initial T = 273.15 K, p = 266.644 Pa, $\lambda = 24\ \mu m$
- Walls: L = 1 mm = 42λ, $\Delta T = 70$ K, $\Delta V = 100$ m/s
- $N_c = 120$, $\Delta t = 7$ ns, $\Delta x = 2.5$ mm, ~10^9 samples/cell, 32 runs

Small velocity slips, temperature jumps, Knudsen layers

DSMC Reproduces Infinite-Approximation Chapman-Enskog Transport Coefficients

Sandia National Laboratories

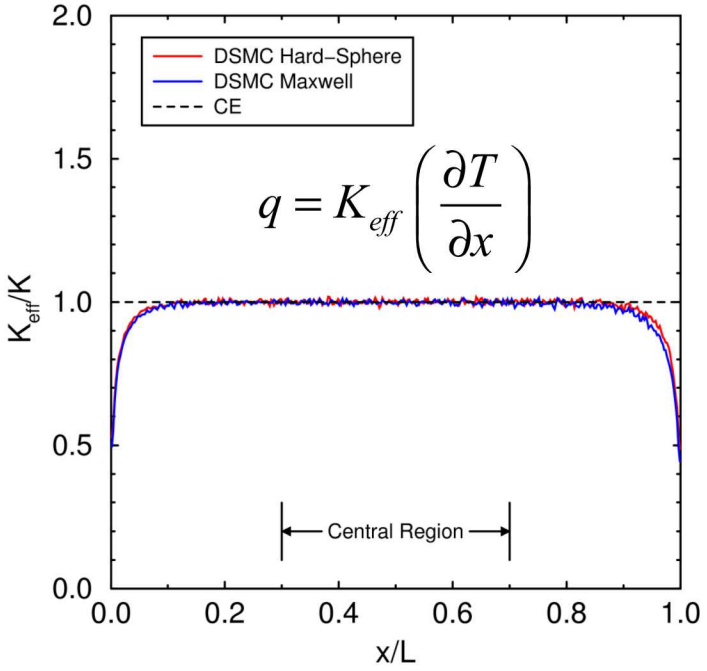

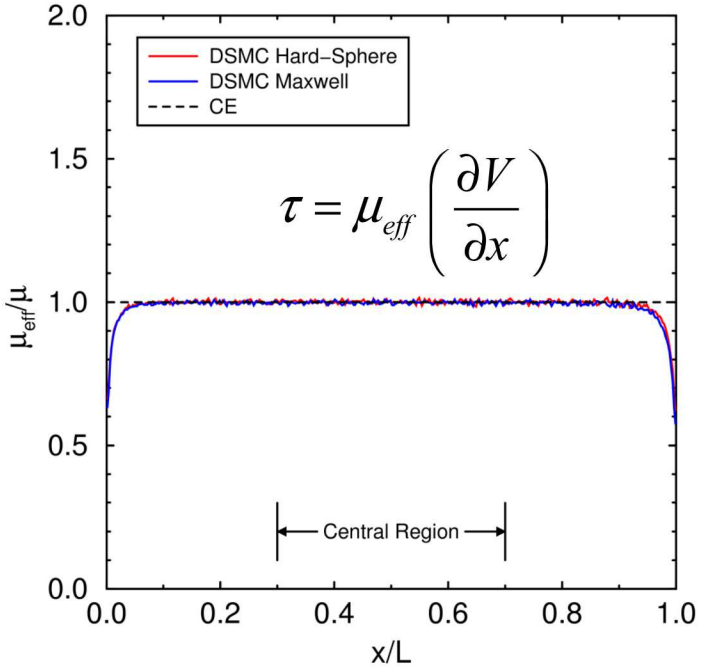

Thermal conductivity (left) and viscosity (right) away from walls

- Maxwell and hard-sphere results bound most gases
- Agreement with Chapman-Enskog theory verifies DSMC

DSMC Reproduces Infinite-Approximation Chapman-Enskog Velocity Distribution

Sandia National Laboratories

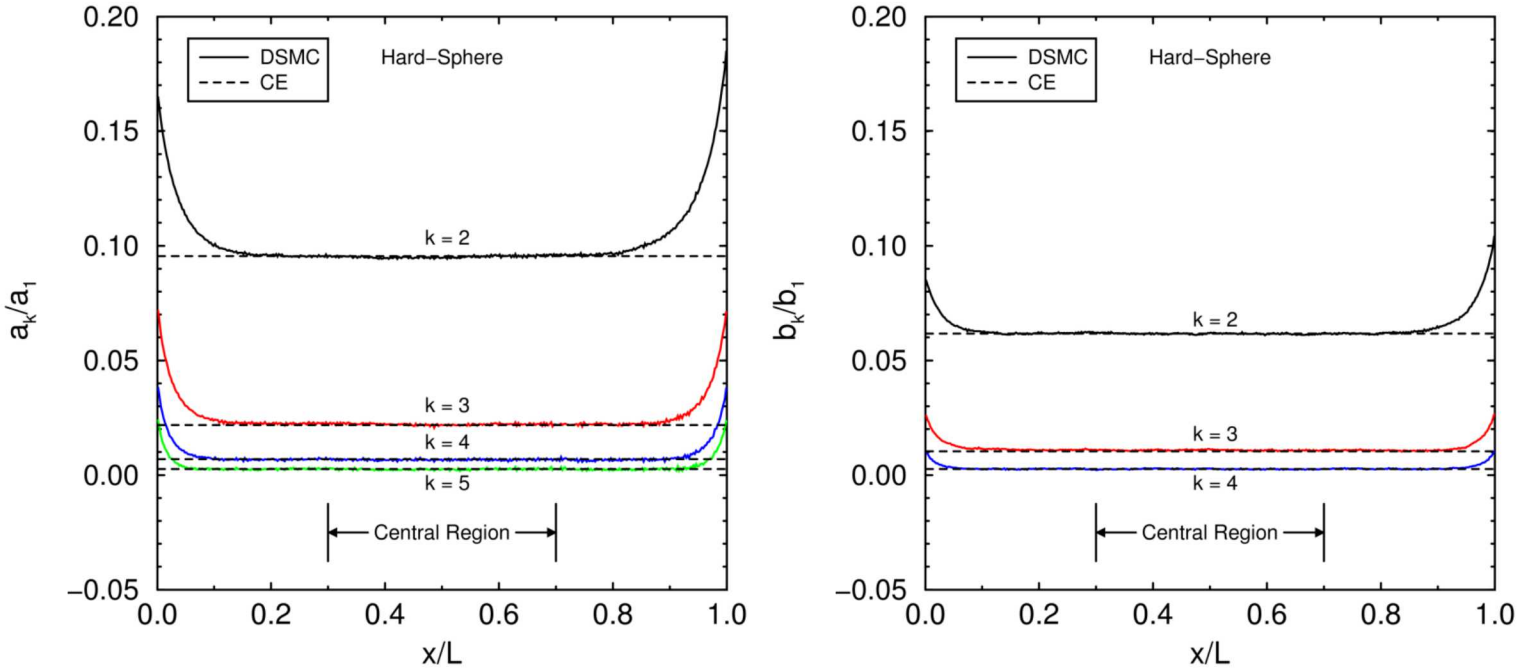

Sonine polynomial coefficients for temperature (left) & velocity (right) gradients

- Hard-sphere values are shown, other interactions have similar agreement
- Higher-order (k > 5) coefficients (not shown) also have similar agreement

Gallis M. A., Torczynski J. R., Rader D. J., "Molecular Gas Dynamics Observations of Chapman-Enskog Behavior and Departures Therefrom in Nonequilibrium Gases", *Physical Review E*, 69, 042201, 2004.

Moment-Hierarchy Method

$$M_{k_1k_2k_3} = \int \tilde{c}_x^{k_1}\tilde{c}_y^{k_2}\tilde{c}_z^{k_3}\tilde{f}[\tilde{\mathbf{c}}]d\tilde{\mathbf{c}} = \left\langle \tilde{c}_x^{k_1}\tilde{c}_y^{k_2}\tilde{c}_z^{k_3}\right\rangle \qquad J_{k_1k_2k_3} = \int \tilde{c}_x^{k_1}\tilde{c}_y^{k_2}\tilde{c}_z^{k_3}J[\tilde{\mathbf{c}}\,|\,\tilde{f},\tilde{f}]d\tilde{\mathbf{c}}$$

$$J_{k_1k_2k_3} = \text{Bilinear}\left[\left\{M_{k_1k_2k_3}\right\}\right] \qquad M_{k_1k_2k_3}[\text{Kn}_q,\text{Kn}_\tau] = \sum_{j=0}^{k_1+k_2+k_3-2} \mu_{k_1k_2k_3}^{(j)}[\text{Kn}_\tau]\text{Kn}_q^j$$

$$K_{\text{eff}}/K = F_K[\text{Kn}_\tau] = 1 - c_K\text{Kn}_\tau^2 + \text{O}[\text{Kn}_\tau^4] \qquad \mu_{\text{eff}}/\mu = F_\mu[\text{Kn}_\tau] = 1 - c_\mu\text{Kn}_\tau^2 + \text{O}[\text{Kn}_\tau^4]$$

$$a_k/a_1 = (-1)^{k-1}\sum_{j=1}^{k-1} A_{kj}\text{Kn}_q^{2j} \qquad b_k/b_1 = (-1)^{k-1}\sum_{j=1}^{k-1} B_{kj}\text{Kn}_q^{2j}$$

Moment-Hierarchy (MH) normal solution

- Solve Boltzmann eqn. recursively for Maxwell molecules
- MH solution extends CE solution to finite Kn_q and Kn_τ
- Collision-term moments bilinear in distribution moments

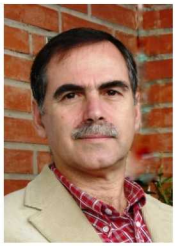

Andres Santos

Compare MH and DSMC for Maxwell molecules

- Dependence of K, m, a_k/a_1, b_k/b_1 on Kn_q and Kn_τ

Gallis M. A., Torczynski J. R., Rader D. J., Tij M., Santos A., "Normal Solutions of the Boltzmann Equation for Highly Nonequilibrium Fourier and Couette Flow", *Phys. Fluids, 18, 017104,* 2006.

Maxwell Normalized Sonine Coefficients

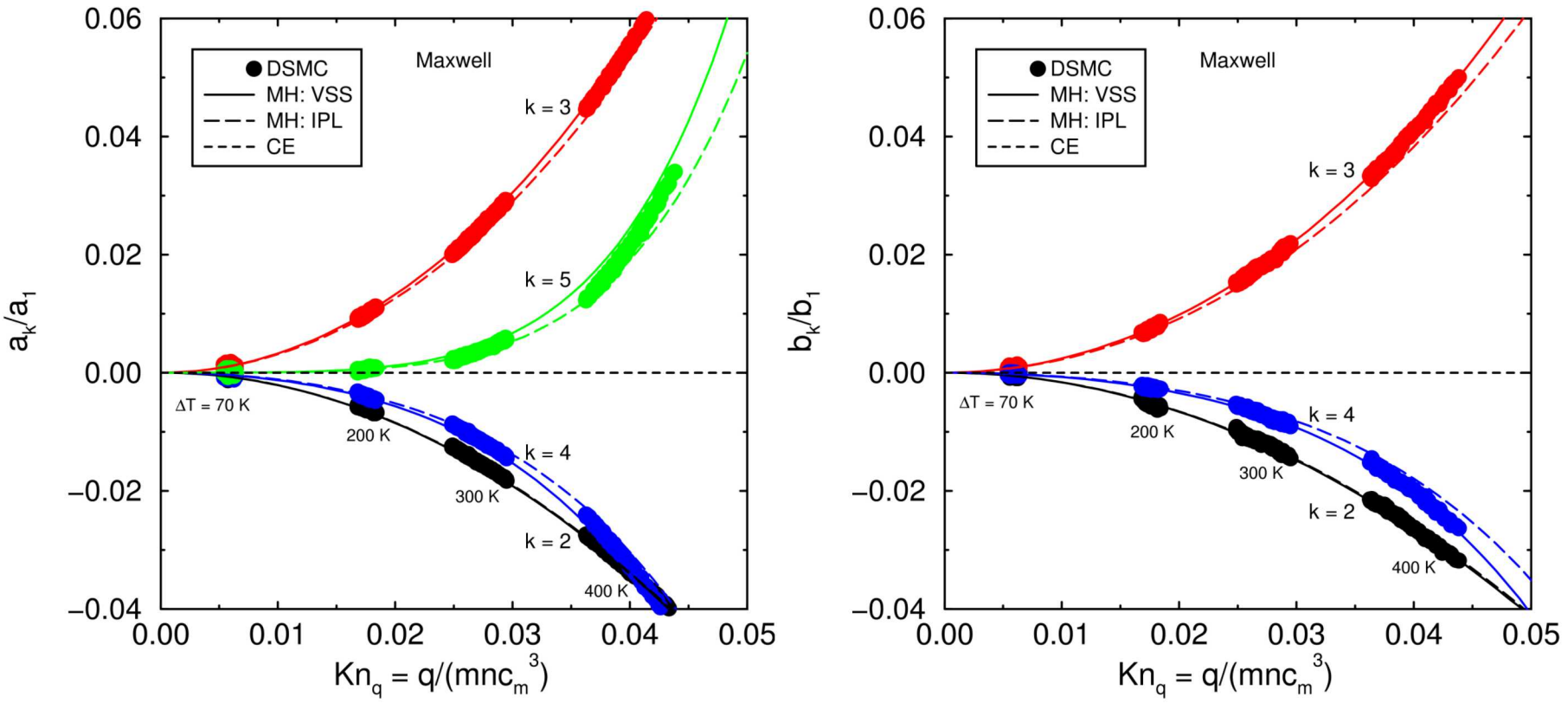

DSMC and MH Maxwell normal solutions for a_k/a_1 and b_k/b_1

- Four DSMC simulations: ΔT = 70, 200, 300, 400 K
- MH: VSS-Maxwell (solid) and IPL-Maxwell (dashed) differ
- DSMC and MH VSS-Maxwell normal solutions agree

Maxwell Normal Transport Coefficients

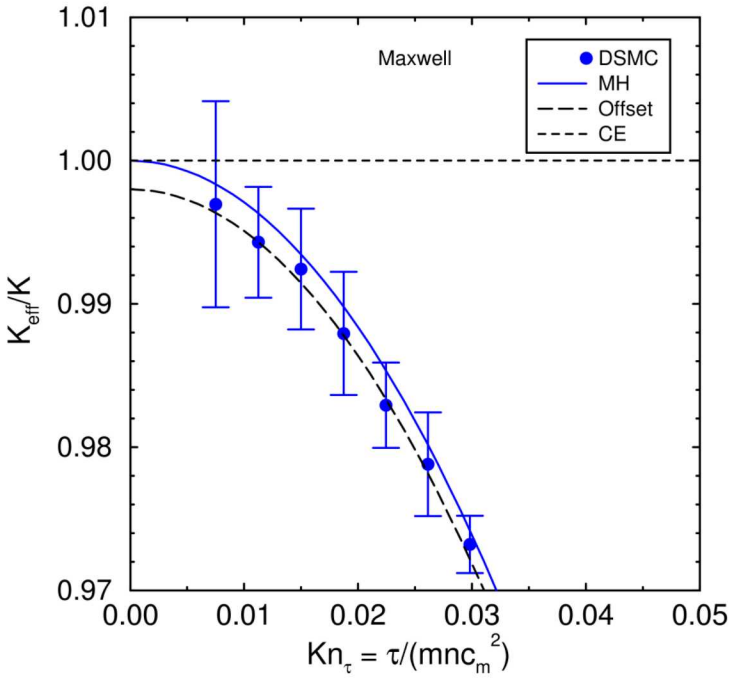

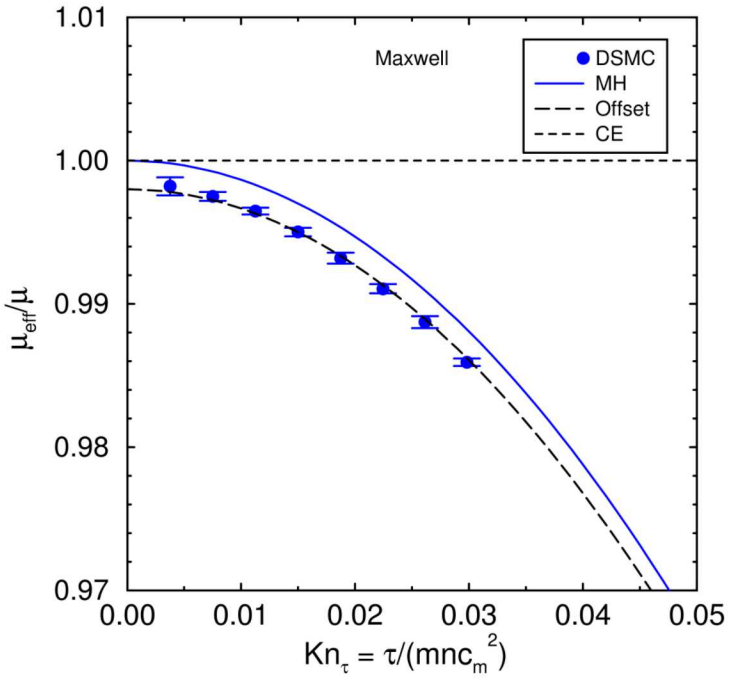

DSMC and MH Maxwell normal solutions for K and m

- Finite Kn_t (shear stress), low Kn_q (heat flux)
- Eight DSMC simulations: ΔV = 100, …, 800 m/s
- Thermal conductivity from viscous heating, larger errors
- Offset MH by DSMC discretization error

Agree to within DSMC discretization error

Parallel Efficiency: The Unfair Advantage

Sandia National Laboratories

- The advantages of DSMC come at a cost
- DSMC is computationally efficient but computationally intense
- Its successful application to real problems depends heavily on its parallel performance

- 1000x speedup required for some problems of interest
- Monte Carlo methods usually have good parallel performance
    - The workload depends mainly on the molecules within a cell
    - Relatively less need to communicate information between cells
    - Trivial to parallelize in velocity space

The necessary speedup can be achieved without any loss of accuracy or convergence characteristics through parallel computing

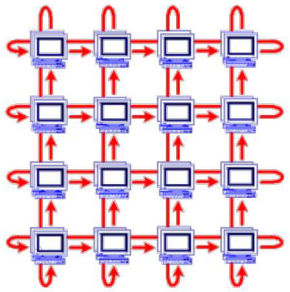

=

Top 5 Supercomputers (2014)

Sandia National Laboratories

Rank	Site	System	Cores	Rmax (TFlop/s)	Rpeak (TFlop/s)
1	National Super Computer Center in Guangzhou	**Tianhe-2 (MilkyWay-2)** - TH-IVB-FEP Cluster, Intel Xeon E5-2692 12C 2.200GHz, TH Express-2, Intel Xeon Phi 31S1P	3,120,000	33,862.7	54,902.4
2	DOE/SC/Oak Ridge National Laboratory	**Titan** - Cray XK7 , Opteron 6274 16C 2.200GHz, Cray Gemini interconnect, NVIDIA K20x	560,640	17,590.0	27,112.5
3	DOE/NNSA/LLNL	**Sequoia** - BlueGene/Q, Power BQC 16C 1.60 GHz, Custom	1,572,864	17,173.2	20,132.7
4	RIKEN Advanced Institute for Computational Science (AICS)	**K computer**, SPARC64 VIIIfx 2.0GHz, Tofu interconnect	705,024	10,510.0	11,280.4
5	DOE/SC/Argonne National Laboratory	**Mira** - BlueGene/Q, Power BQC 16C 1.60GHz, Custom	786,432	8,586.6	10,066.3

24h hr run on Sequoia = 4,310 years CPU time

Programming for Next Generation and Exascale Machines

Sandia National Laboratories

Goal is to decouple the science code from the hardware details

Envisaged Next Generation Platforms:

- Millions of nodes likely
- Reduced memory per node
- Parallelism within node:
  - Multi-core: 16 and growing
  - Many-core: Intel Xeon Phi, 240 threads
  - GPUs: NVIDIA/AMD, 1000 warps

- **Example**: LLNL BG/Q: 96K nodes, 16 cores/node + 4 MPI tasks/core

Necessary elements

- Adaptive gridding
- In-situ visualization
- Efficient communications
- Load balancing

Developing an Exascale DSMC Code

Sandia National Laboratories

SPARTA = Stochastic PArallel Rarefied-gas Time-accurate Analyzer

General features

- 2D or 3D, serial or parallel
- Cartesian, hierarchical grid
  - Oct-tree (up to 16 levels in 64-bit cell ID)
  - Multilevel, general NxMxL instead of 2x2x2
- Triangulated surfaces cut/split the grid cells
  - 3D via Schwartzentruber algorithm
  - 2D via Weiler/Atherton algorithm
  - Formulated so can use as kernel in 3D algorithm
- C++, but really object-oriented C
  - Designed to be easy to extend
  - New collision/chemistry models, boundary conditions, etc.

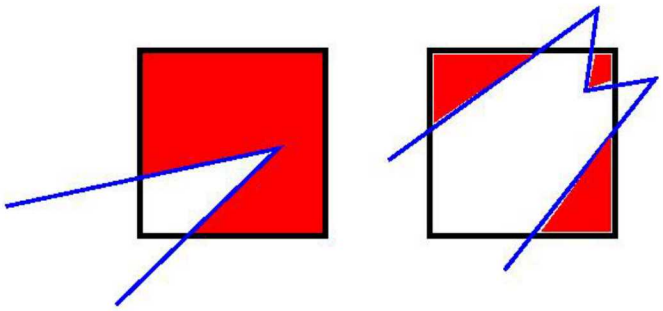

- Code available at http://sparta.sandia.gov

Simulation of Complicated Shapes

Sandia National Laboratories

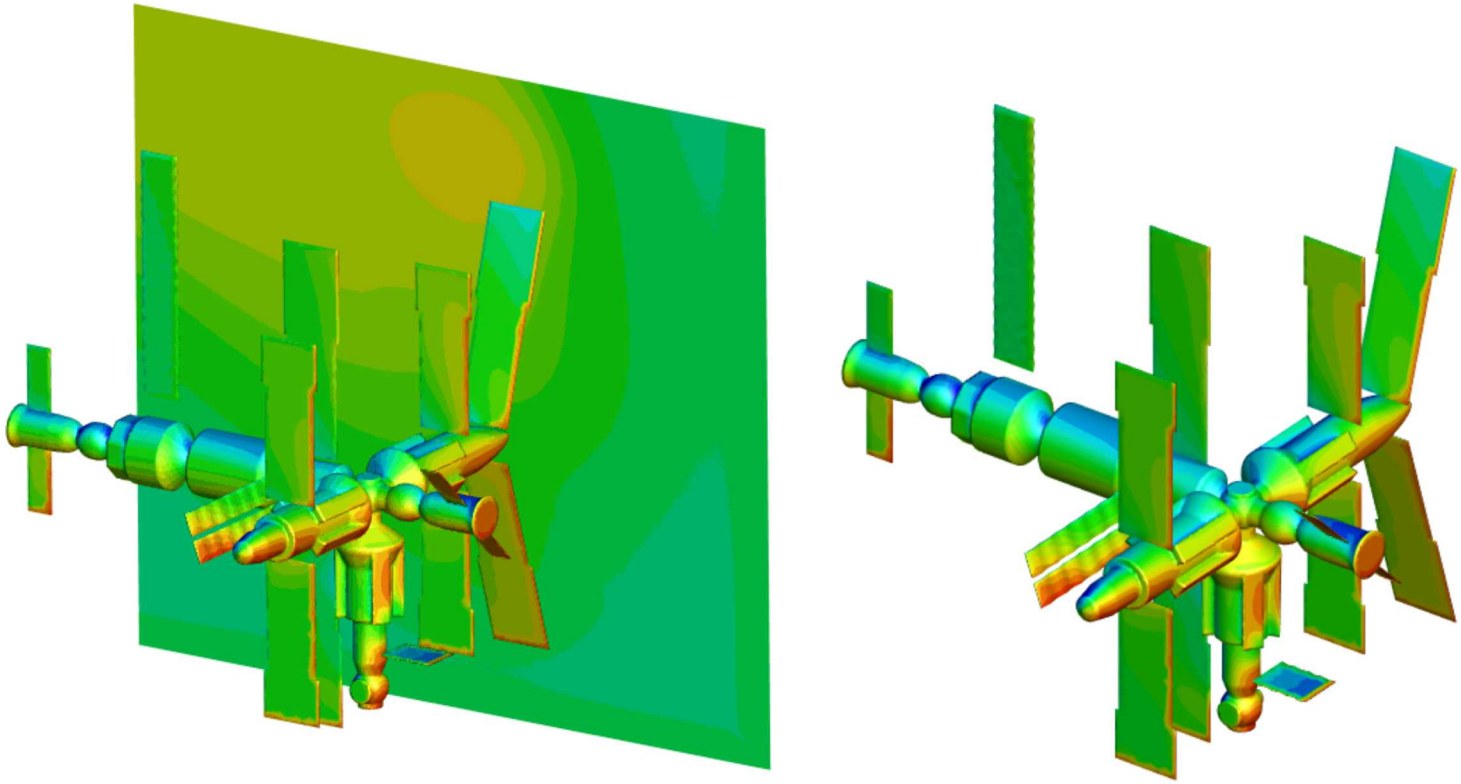

Mir Space Station

Grid generation (10^7 cells) completed in 0.3 seconds on 16 processors
Geometry comprises multiple “water-tight” bodies

Efficient Communication & Load Balancing

Sandia National Laboratories

To achieve maximum efficiency:

- One communication per step
  - Multiple passes if needed (or can bound molecule move)
- Communication with modest count of neighbor processors

- One processor = compact clump of cells via load balancing
  - Ghost region = nearby cells within user-defined cutoff
  - Store surface information for ghost cells to complete move

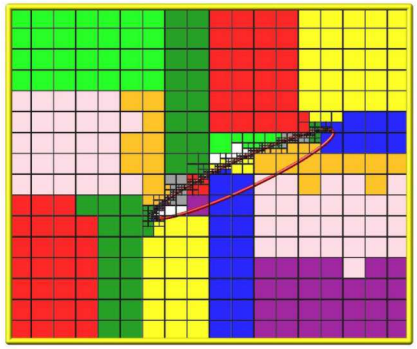

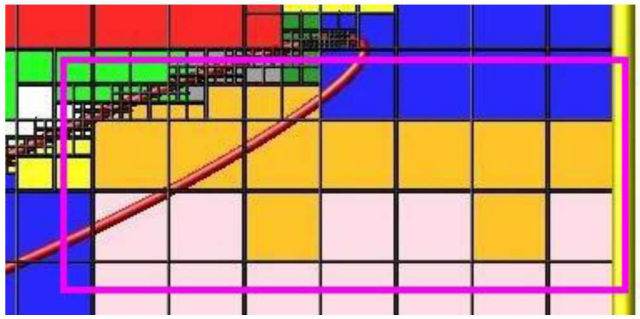

Example:
1B cells on1024 BG/Q node
Worst case: move all cells
Balance time = 15 s:
(RCB=2, move=12, ghosts=1)

- Balance across processors, static or dynamic
- Geometric method: recursive coordinate bisection (RCB)
- Weighted by cell count or molecules or CPU

In-Situ Visualization

Sandia National Laboratories

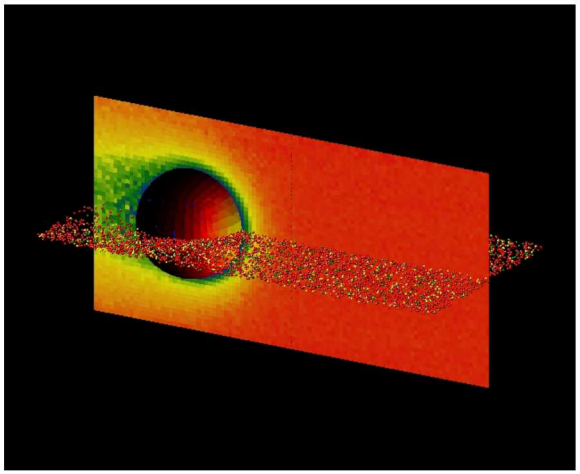

Not a replacement for interactive viz, but ...
Quite useful for debugging & quick analysis
At end of simulation (or during), instant movie

Render a JPG snapshot every N time steps:

- Each processor starts with blank image (1024x1024)
- Processor draws its cells/surfaces/molecules with depth-per-pixel
- Merge pairs of images, keep the pixel in front, recurse
- Draw is parallel, merge is logarithmic (like MPI Allreduce)

Images are ray-traced quality

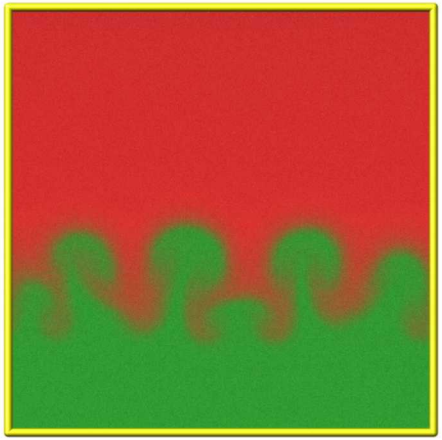

SPARTA Benchmarking

Sandia National Laboratories

- Flow in a closed box
  - Stress test for communication
    - No preferred communication direction
  - 3D regular grid, 10^4-10^{11} (0.1 trillion) grid cells
  - 10 molecules/cell, 10^5-10^{12} (1 trillion) molecules
- Effect of threading
  - 2 threads/core = 1.5 speed
  - 4 threads/core = 2x speed

SPARTA Benchmarking

Sandia National Laboratories

16 cores/node
1 task/core

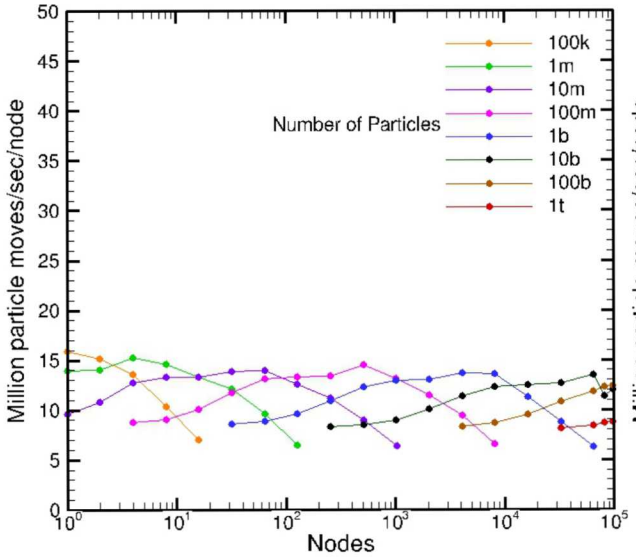

16 cores/node
2 tasks/core

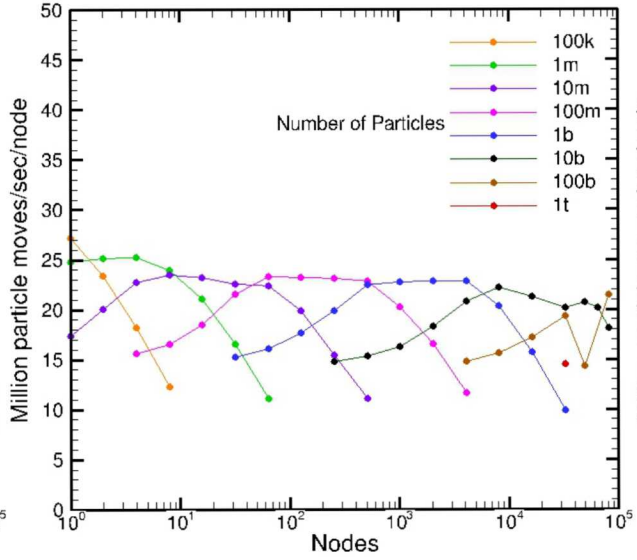

16 cores/node
4 tasks/core

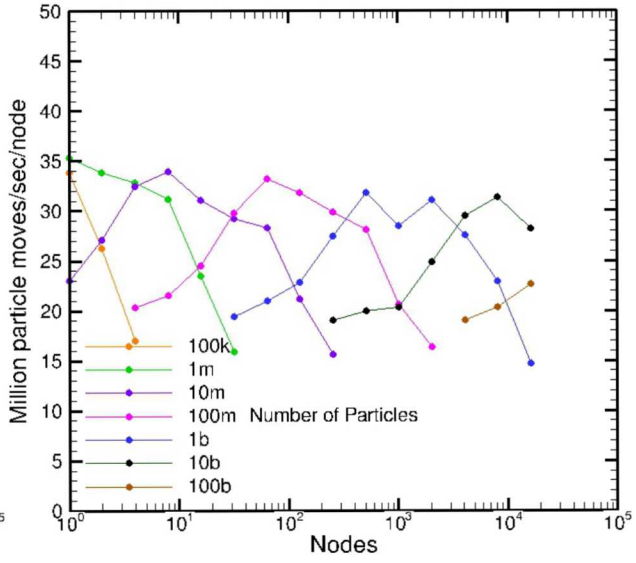

- Weak scaling indicates, 10% peak performance reduction from 1 to 10^6 cores
- 2 tasks/core gives 1.5x speedup, 4 tasks/core gives 2x speedup
- A total of 1 trillion molecules can be simulated on one third of the BG/Q
- Maximum number of tasks is 2.6 million

The Rayleigh-Taylor Instability

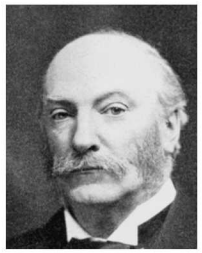

Baron Rayleigh

G.I. Taylor

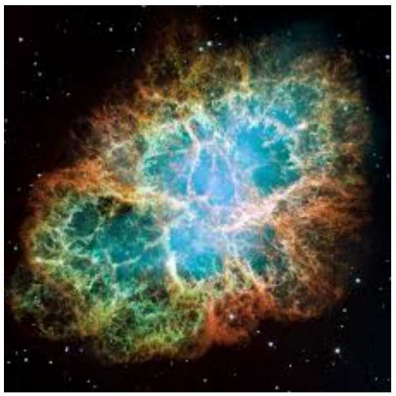

RTI is an interfacial instability that occurs when a high-density fluid is accelerated or supported by a low density one.

Small deviations from planarity (or sphericity) amplify with time and eventually lead to mixing.

The growth of the instability is influenced by viscosity, compressibility, three-dimensionality, density ratio

It is postulated that the failure to achieve ignition at NIF can be attributed to RTI.

Applications range from ICF (mm) to formation of supernova remnants (light-years).

Why DSMC for Rayleigh-Taylor Instability?

Sandia National Laboratories

- DSMC provides a molecular-level description of the hydrodynamic processes that may be physically more realistic for **large accelerations and chemically reacting flows**
- DSMC inherently accounts for transport properties
- The DSMC method offers the potential to identify the impact of molecular level effects (e.g. rotational and vibrational energy exchange, gas-phase chemical reactions, and gas-surface interactions) on hydrodynamic instabilities.
- Typical DSMC simulation characteristics:
  - Physical Domain: 1 mm x 4 mm (ICF-pellet size domain)
  - # Cells: 4 billion
  - # Particles: 400 billion
  - # Cores: ¼- ½ million
  - Run time: 30hrs (=900, 1800 CPU years)
  - Time steps: 200,000×0.1 ns = 20 μs

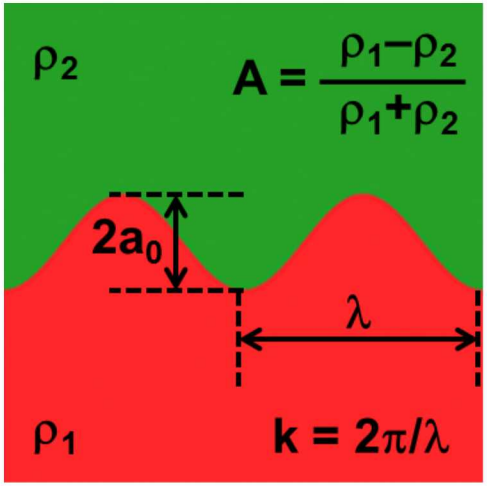

DSMC Simulations of the Rayleigh-Taylor Instability in Gases

Sandia National Laboratories

- The interface between argon (red) and helium (green) gases is slightly perturbed:
  $\lambda = 0.001m, a = 0.00001m$
- Initial state hydrodynamic equilibrium
- Acceleration of the system excites the RTI
  - Initially, thermal fluctuations and diffusion perturb the interface
  - The initial perturbation amplitude grows exponentially
  - A second growth stage occurs at the most unstable wavelength, also forming "**bubbles**" and "**spikes**"
  - Additional instabilities breakup the larger structures, resulting in turbulent and chaotic mixing of the gases

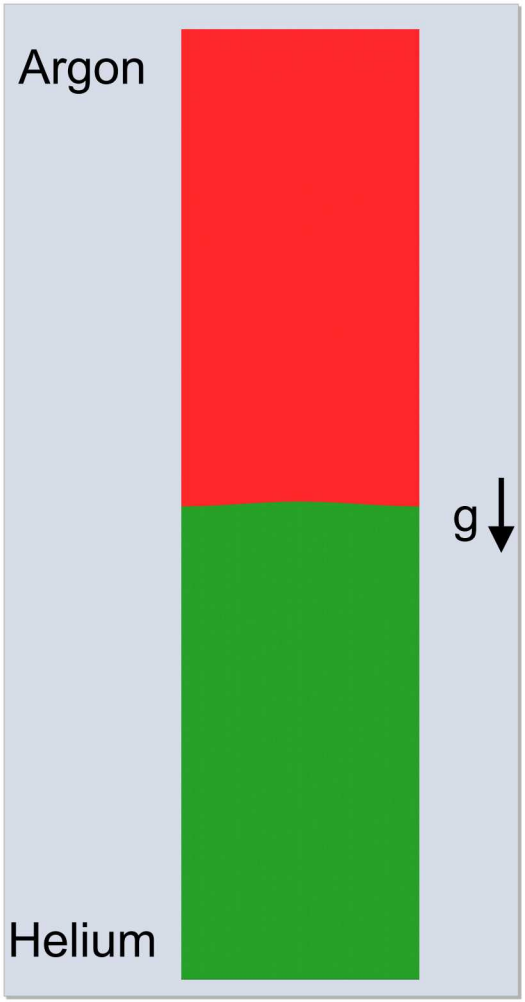

Development of 0.001 m Wavelength Perturbation

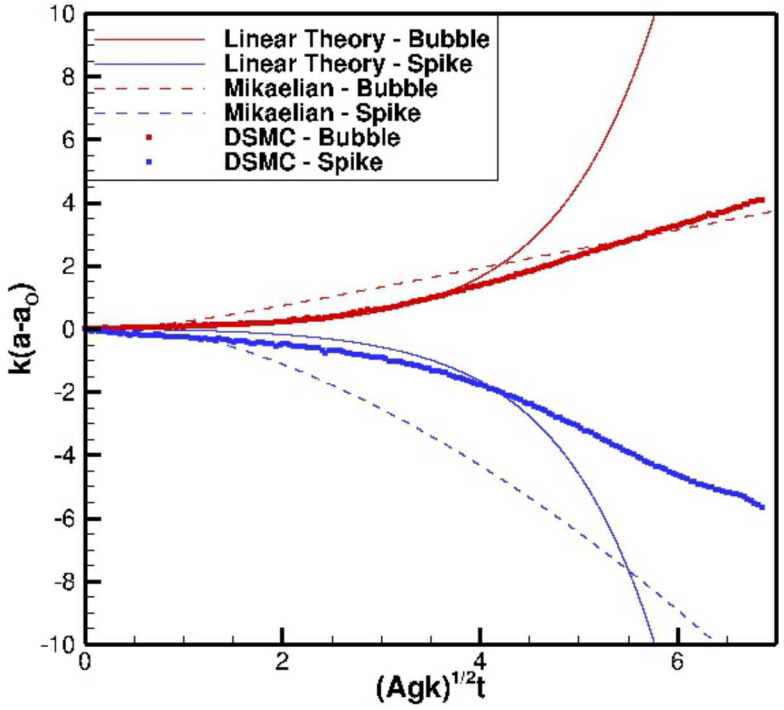

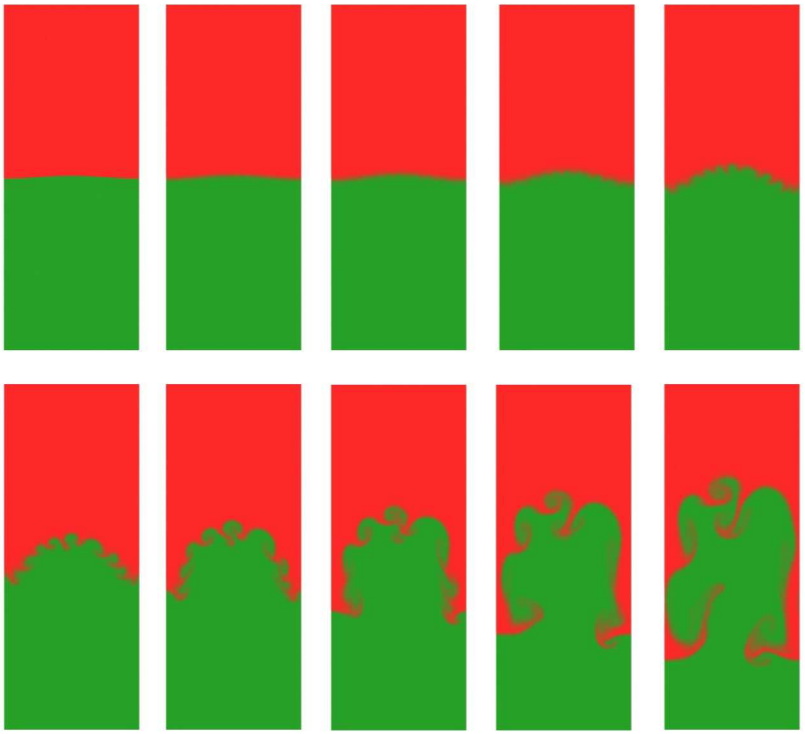

Initial perturbations of a small wavelength develop and grow exponentially. Larger structures appear as the smaller disturbances interact and combine. The structures themselves develop instabilities like the Kelvin-Helmholtz instability, which eventually break up the structures, resulting in turbulent and chaotic mixing of the fluids.

Development of 0.0005 m Amplitude Perturbation

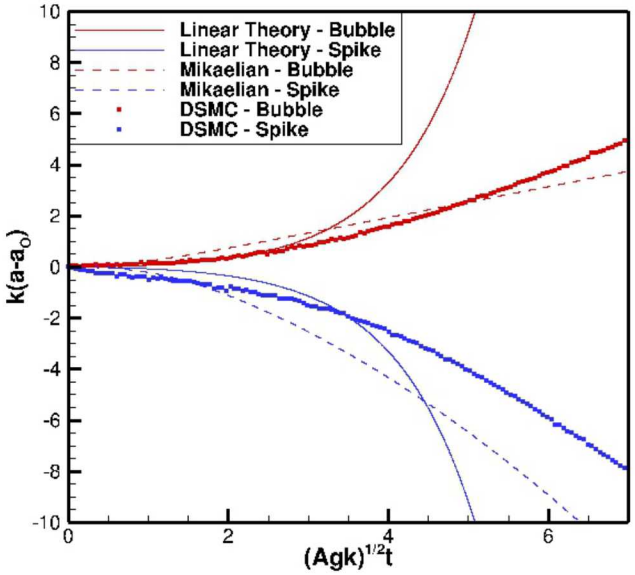

Reasonable agreement with linear theory for small amplitudes

Qualitative agreement with Mikaelian's model for linear and non-linear regimes

Development of 0.0001 m Amplitude Perturbation

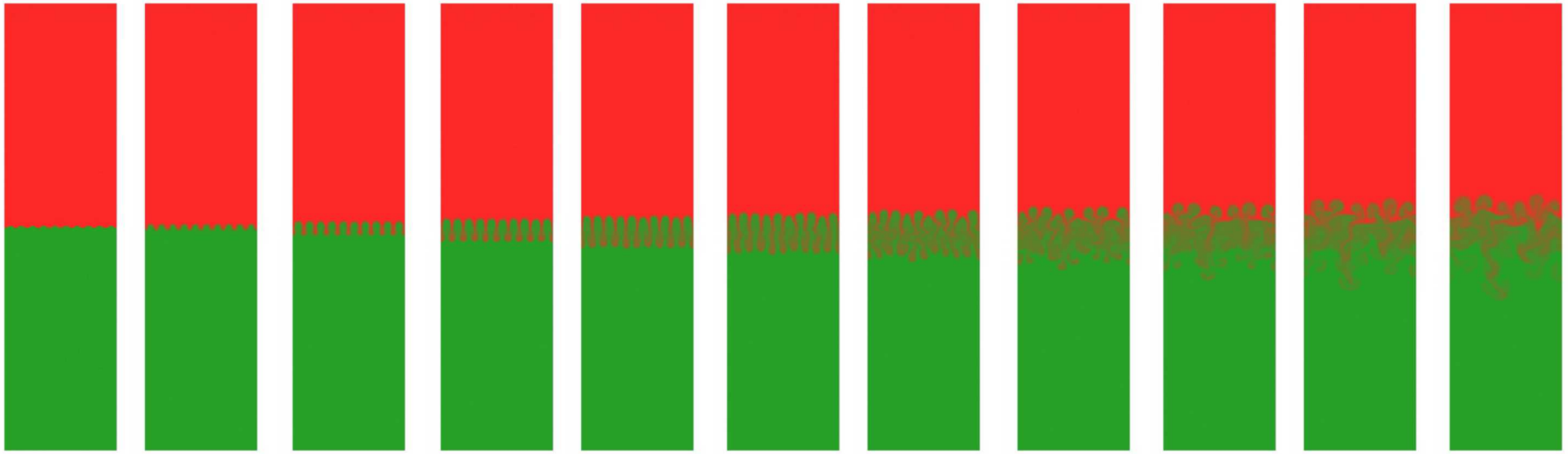

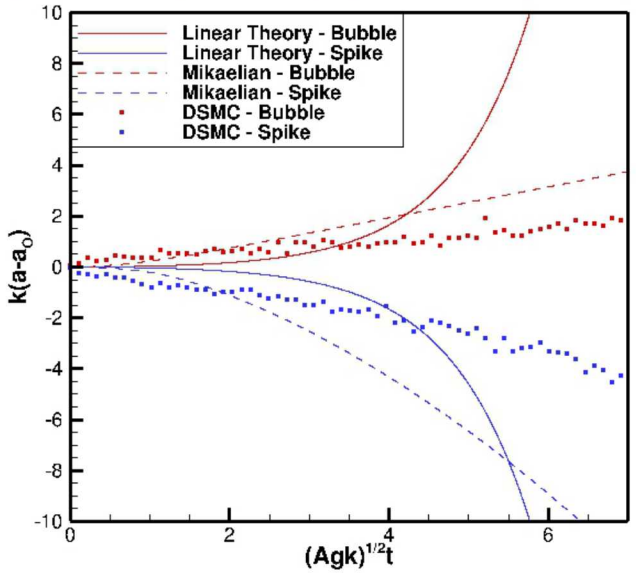

Reasonable agreement with linear theory for small amplitudes

Qualitative agreement with Mikaelian's model for linear and non-linear regimes

RTI: Effect of Atwood Number

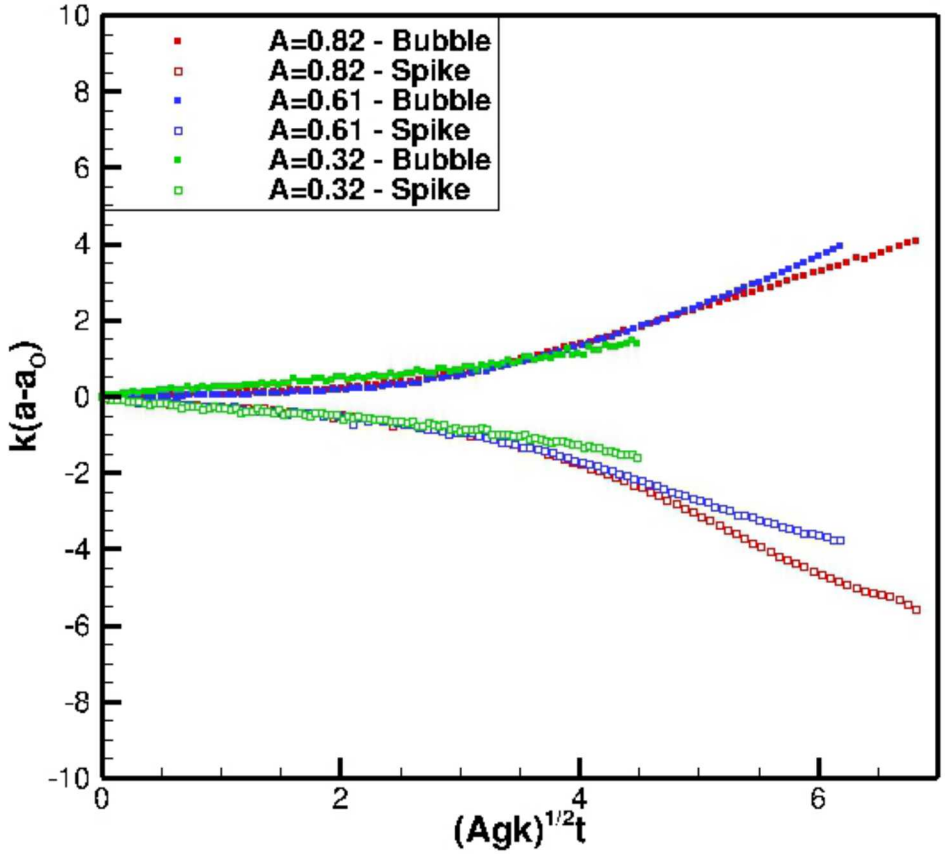

The effect of Atwood number becomes significant in the non-linear region

RTI: Effect of Gravity

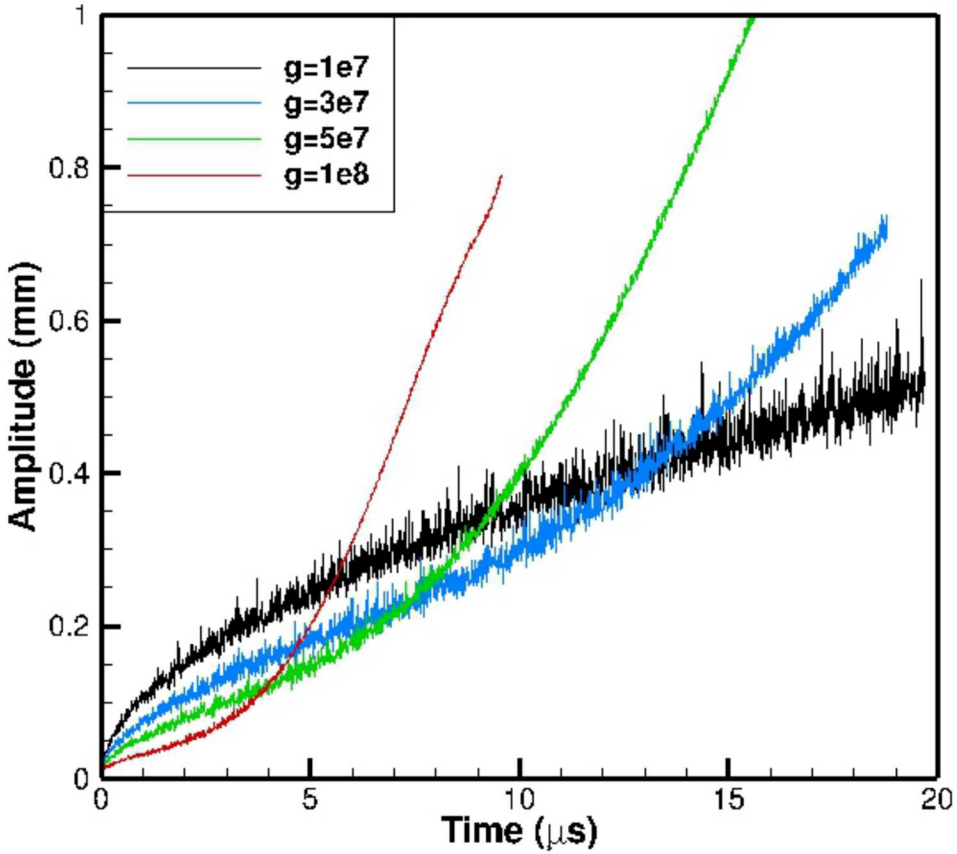

Initially the interface grows due to diffusion followed by exponential (linear regime) and non-linear growth

RTI from an Initially Molecularly Flat Interface

Sandia National Laboratories

- The interface between Argon (red) and Helium (green) gases is initially flat
- Acceleration of the system excites the RTI
  - Initially, thermal fluctuations and diffusion perturb the interface
  - The amplitude of thermal fluctuations exponentially
  - Gases penetrate each other differently, forming "**bubbles**" and "**spikes**"
  - Finally, additional instabilities breakup the larger structures resulting in turbulent and chaotic mixing of the gases

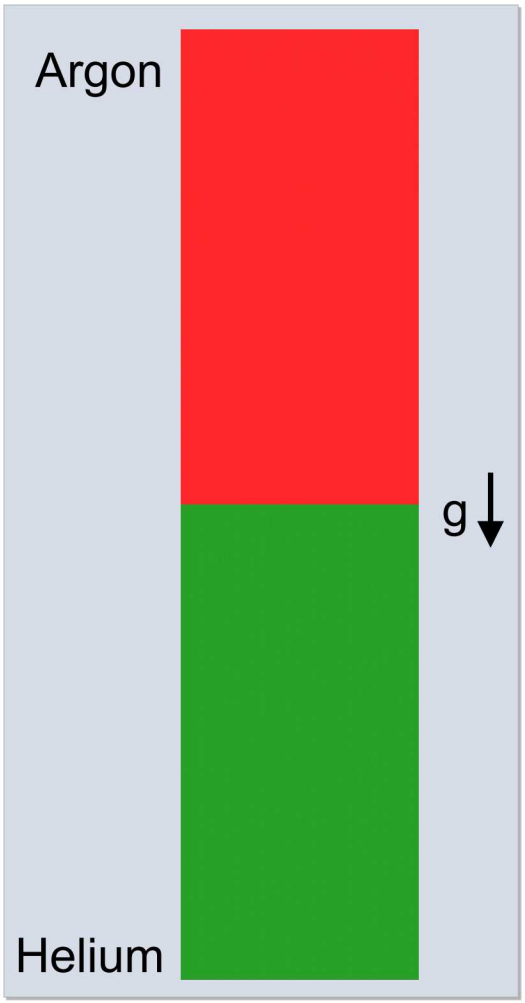

RTI from an Initially Flat Interface

Sandia National Laboratories

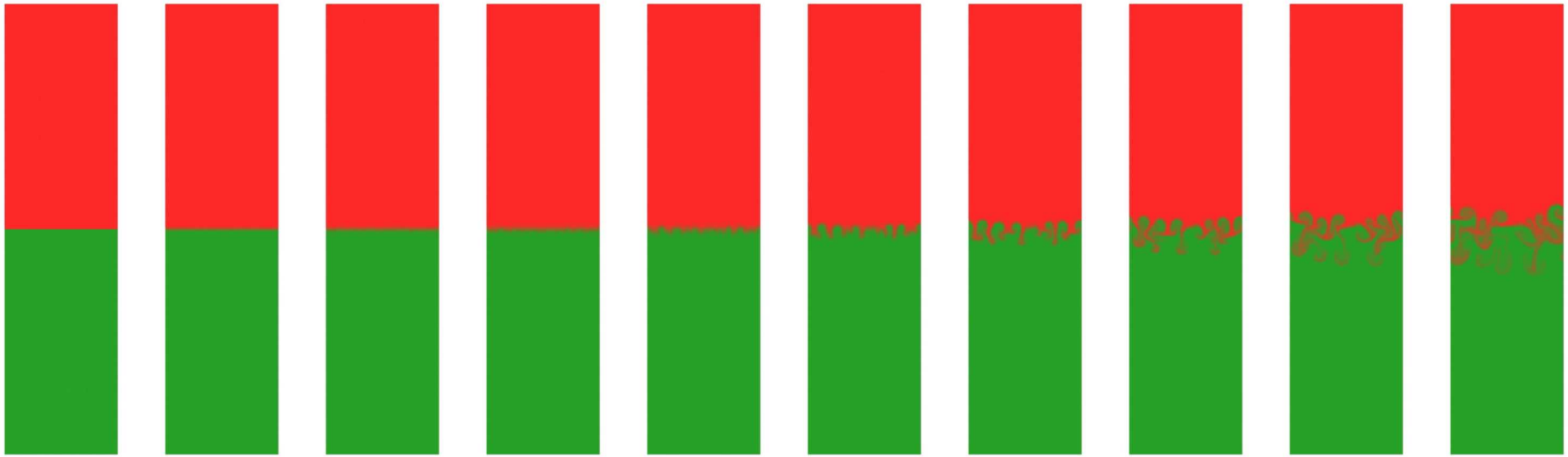

Images progress at 10,000 time step increments

The number of bubbles and spikes correspond to the most unstable wavelength

Richtmyer-Meshkov Instability (RMI)

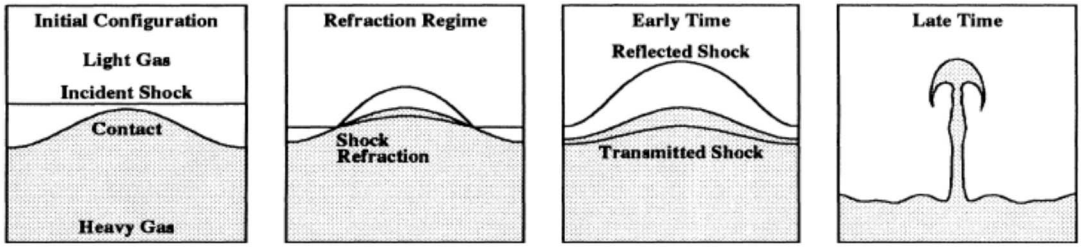

Grove et al., Phys. Rev. Lett., 71(21), 3473 (1993).

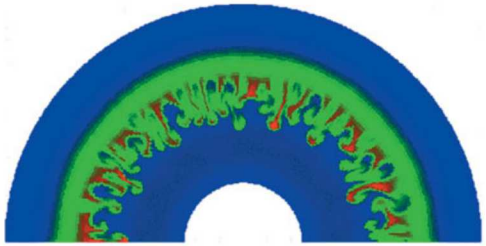

ICF target compression

RMI applications include stellar evolution, inertial confinement fusion, shock-flame interaction

RMI combines multiple fluid-flow phenomena

- Shock transmission and reflection
- Hydrodynamic instabilities
- Linear and nonlinear growth
- Diffusion and turbulent mixing
- Compressibility effects
- Chemical reactions

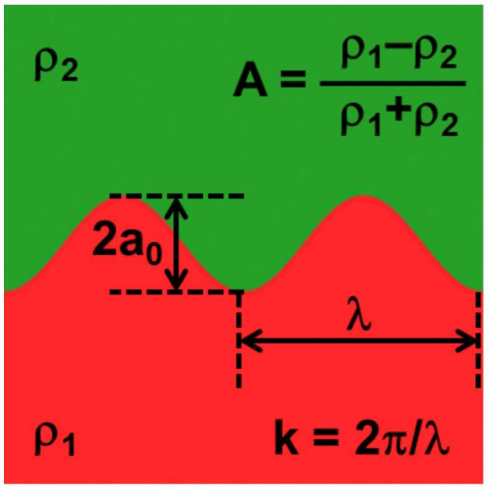

RMI basic geometry

Simulate RMI using molecular gas dynamics

- Physical conditions that can be achieved
- Computational software & hardware needed

RMI in Gas Mixtures

Sandia National Laboratories

Physical situation

- Gases: pairs of helium, neon, argon, xenon, air, SF_6
- STP conditions: both gases at 1 atm and 0 °C
- Two-dimensional domain: 0.1 mm × 0.4 mm
- Wavelength, initial amplitude: 0.05 mm, 0.01-0.1 mm

Numerical parameters

- Mesh: 5 nm, 20,000×80,000 = 1.6 billion cells
- Molecules: 800 billion molecules (500 per cell)
- Time steps: 200,000×0.01 ns = 2 μs

Computational aspects

- Platform: Sequoia, 30 hours
- Processors: ~¼ million cores (16k nodes) (900 years CPU time)

Flow phenomena

- Flow at top is impulsively started and maintained
- Shock wave propagates down and hits interface
- Transmitted and reflected shock waves depart
- Interface moves down and grows thicker

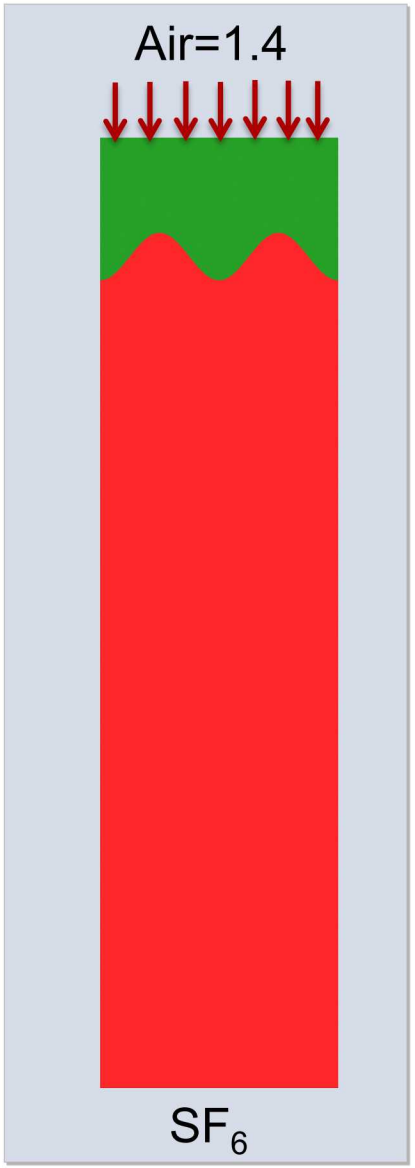

Development of Bubbles and Spikes in RMI

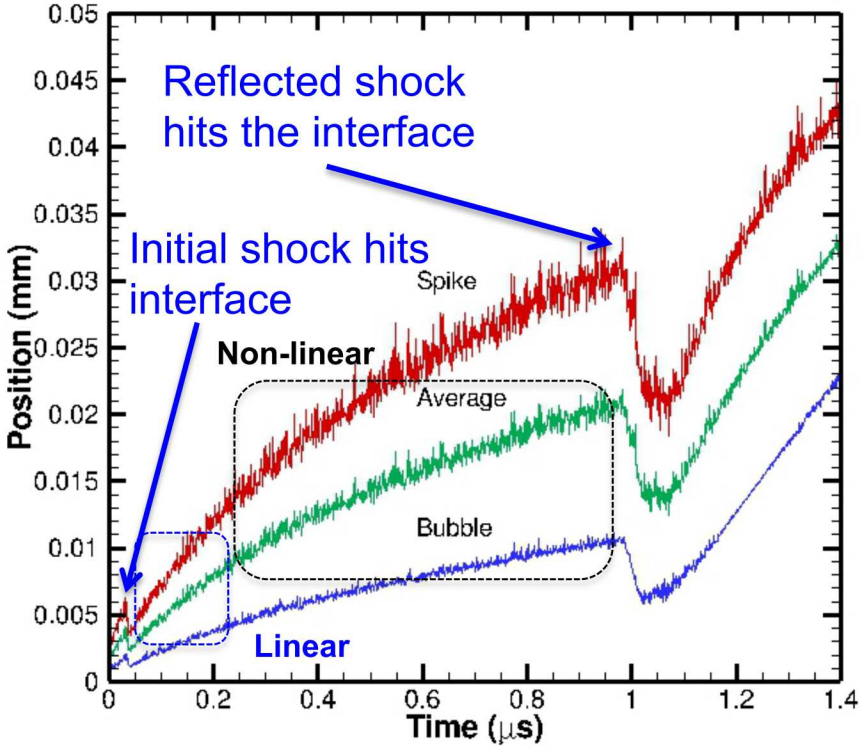

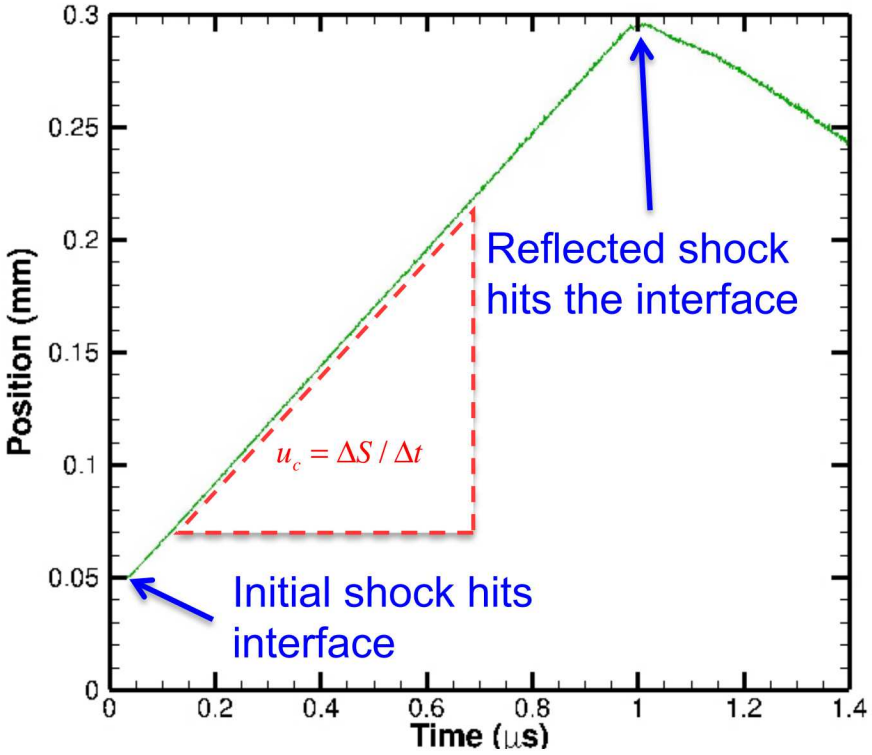

Interface moves with constant speed until the interface gets re-shocked
The development of bubbles and spikes can be tracked independently

RMI in Air-SF_6 Mixture: Mach = 1.4 Shock

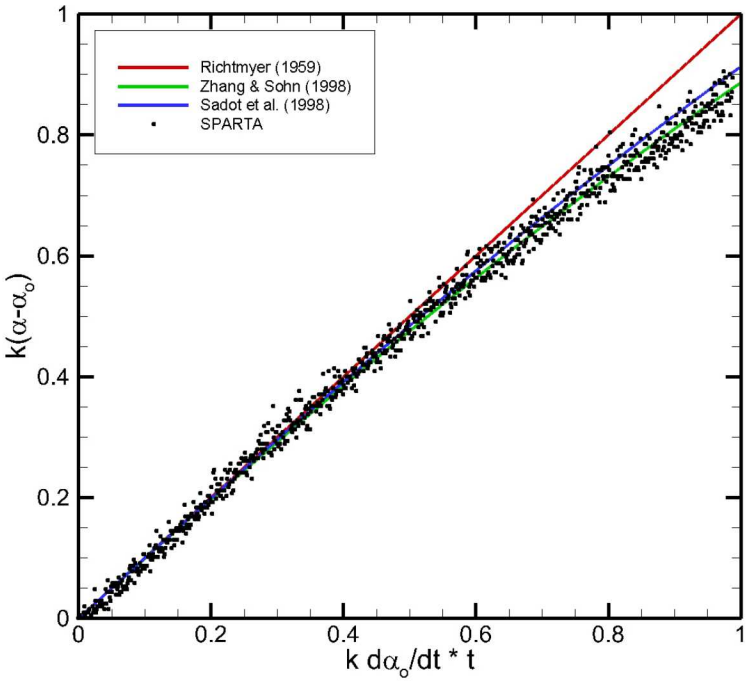

Non-dimensional amplitude for an initially small amplitude perturbation compared to theoretical/empirical models

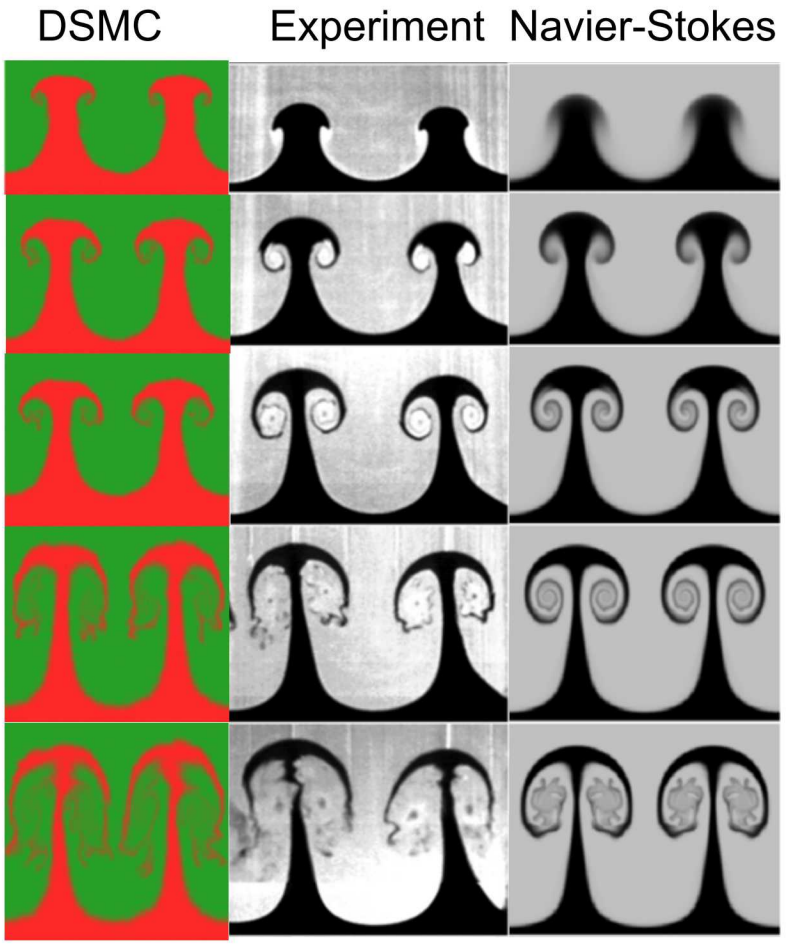

Morgan *et al.* JFM 2012

DSMC-RMI Comparison to Theory

He/Xe
A=0.94

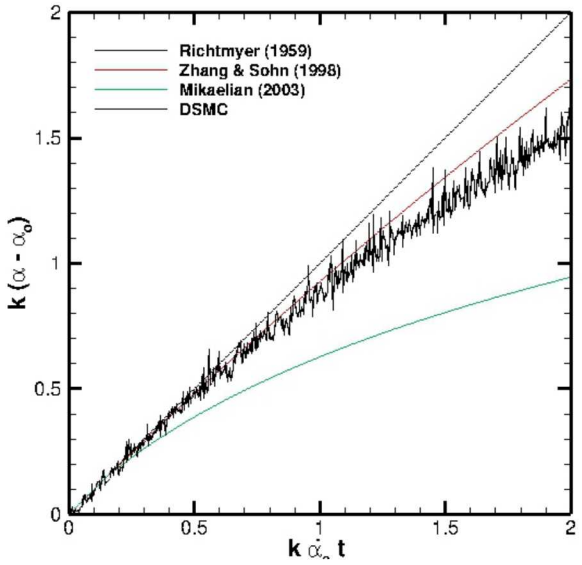

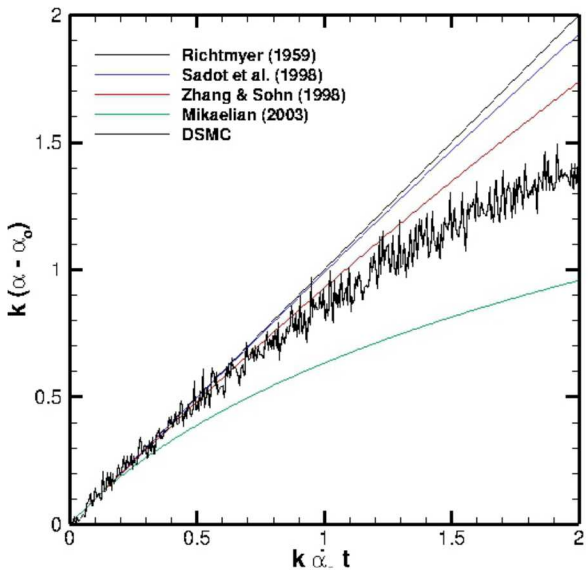

He/Ar
A=0.61

Ar/Xe
A=0.53

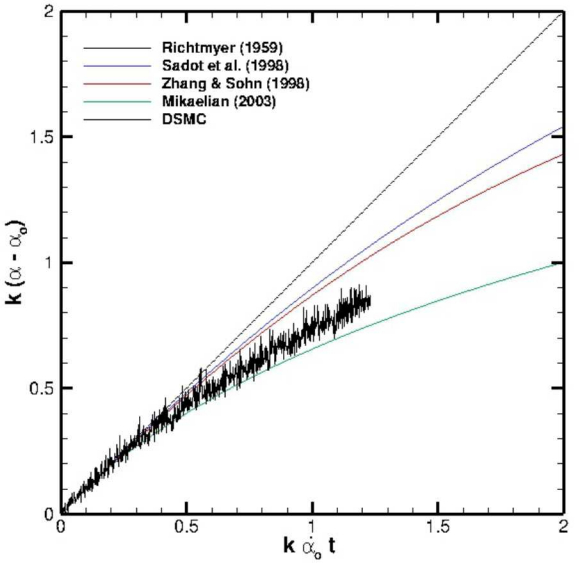

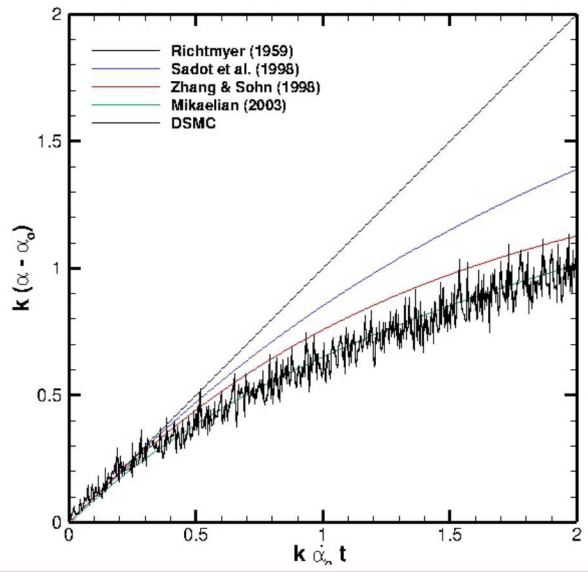

Ne/Ar
A=0.33

RMI: Effect of Atwood Number

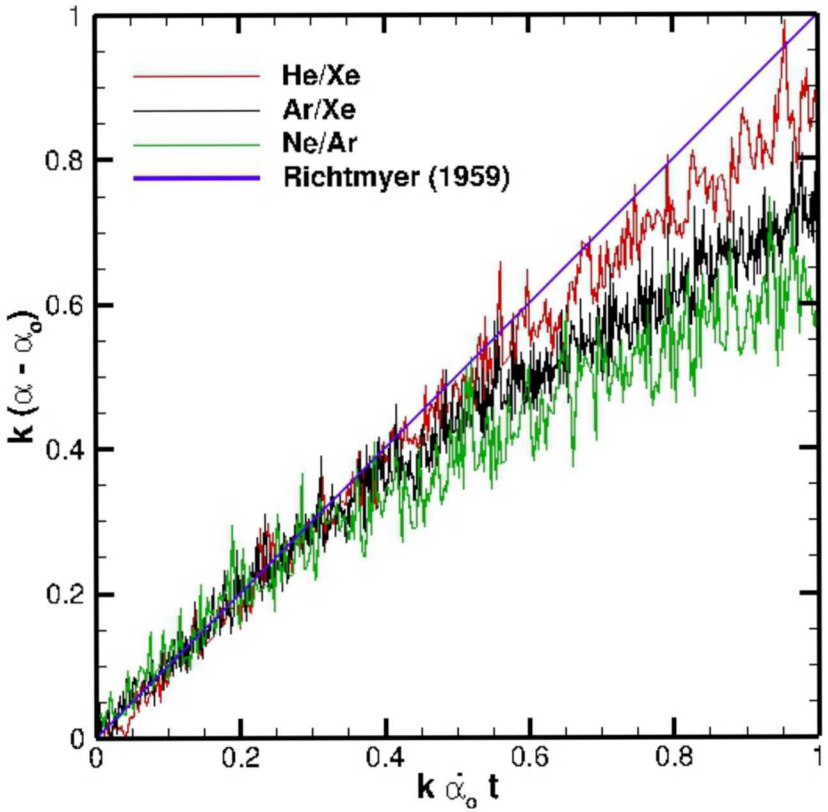

- Different gas pairs give different Atwood numbers in the range 0.33-0.94
- Modest differences are seen over the range examined

RMI: Effect of Mach Number

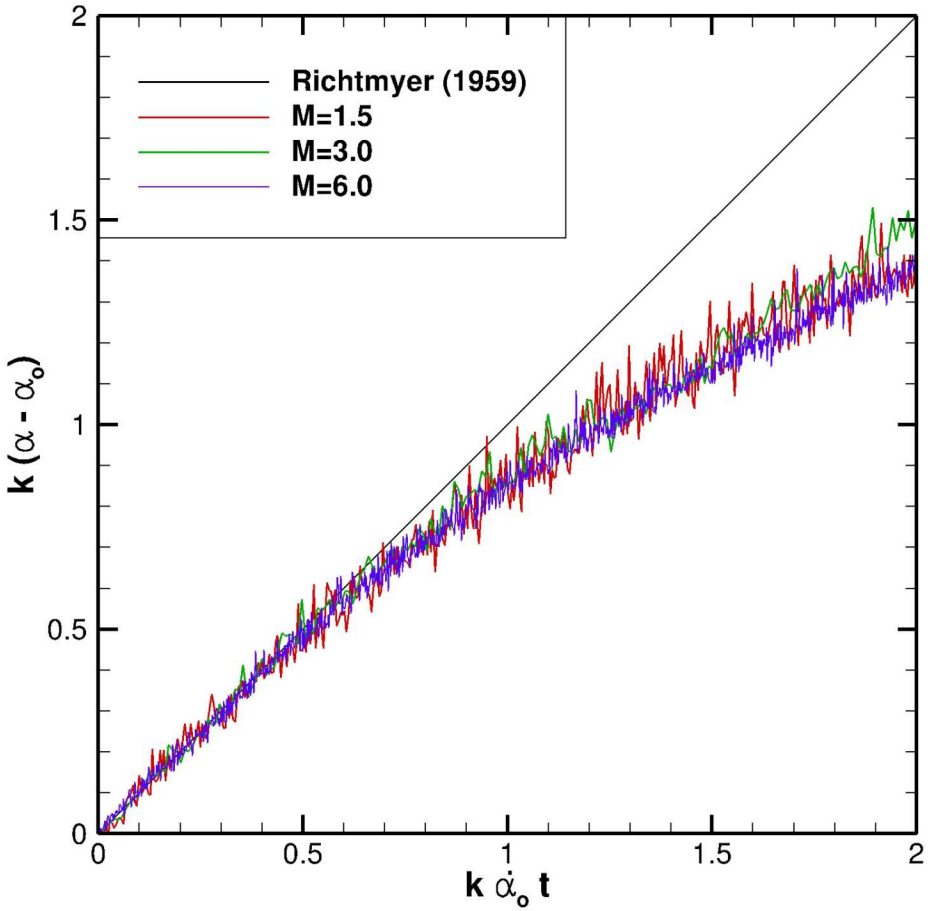

Normalization indicates that Mach number plays a small role

None of the theoretical models accounts for Mach number

Conclusions

DSMC yields exquisite agreement with analytical results, where available

- Chapman-Enskog, Moment-Hierarchy theory

DSMC scales extremely well & can take full advantage of massively parallel platforms

- Can simulate unprecedented flow regimes
- Hydrodynamic instabilities, lower altitudes

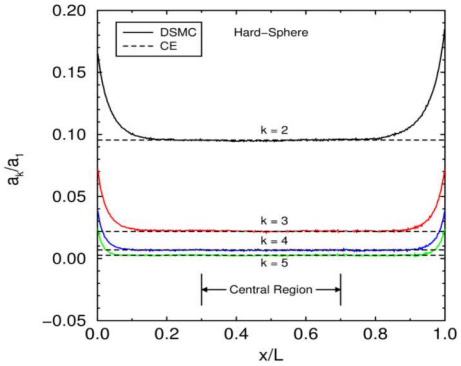

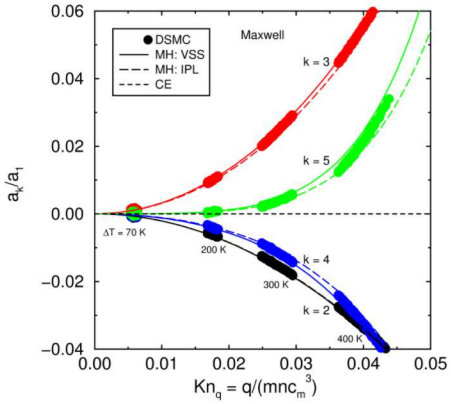

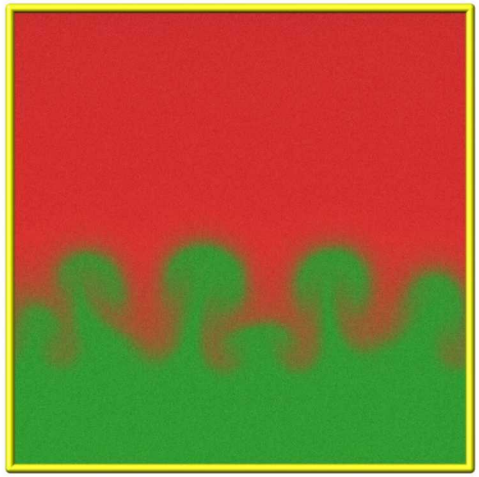

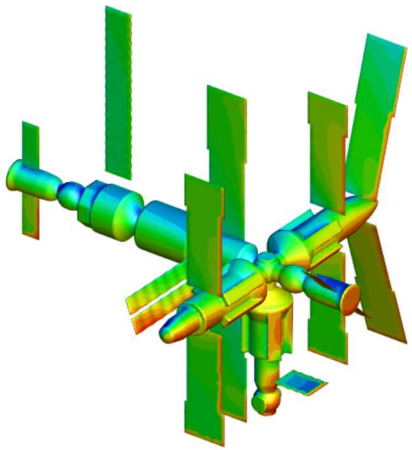

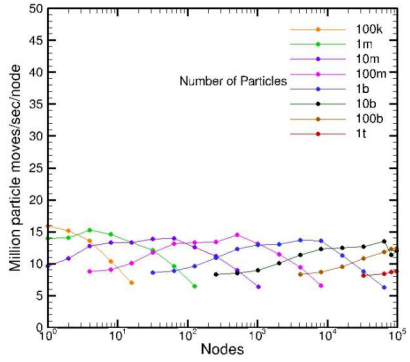

DSMC Numerical Error

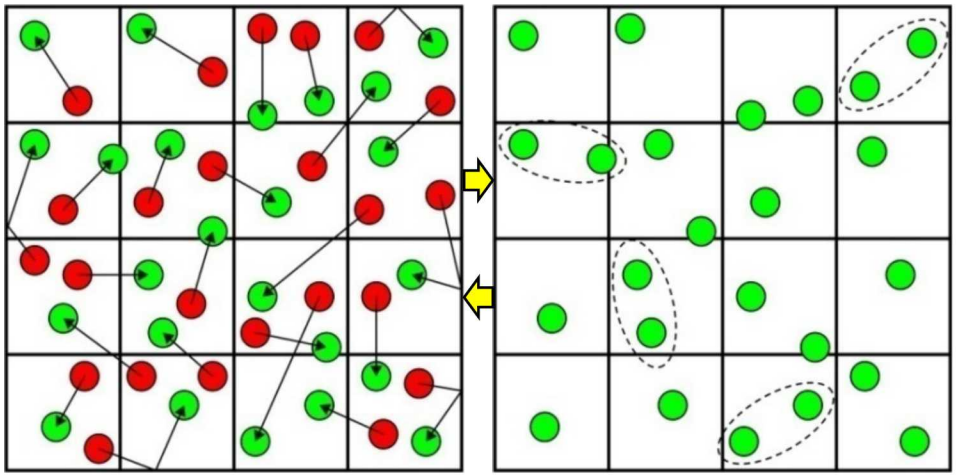

Four parameters control DSMC error:

Statistical error (1)

Samples per cell (S_c)

Discretization error (3)

- Particles per cell (N_c)
- Cell size (Δx)
- Time step (Δt)

Statistical and Particle-Number Errors

Sandia National Laboratories

Error related to sample size

- Statistical error
- Cell sample size $S_c = N_c \times N_t$
- N_c = particles per cell; N_t = time steps

Strategies for overcoming statistical error

- Use large number of samples
- For steady flows, use time and/or ensemble averaging
- Computational expense ~ S_c

Error related to local number of particles

- Error $\sim 1/N_c$
- Systematic – persists even as $S_c \rightarrow \infty$

Limited number of samples per time step

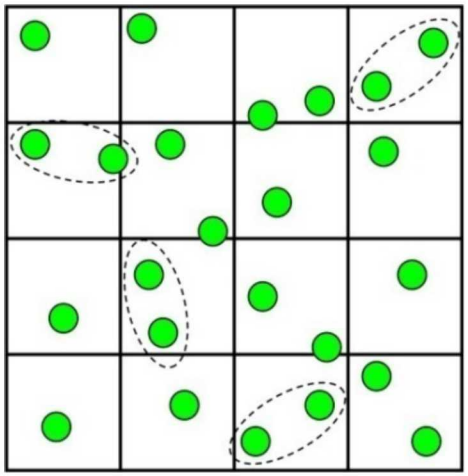

Not enough particles to capture physics

DSMC Convergence

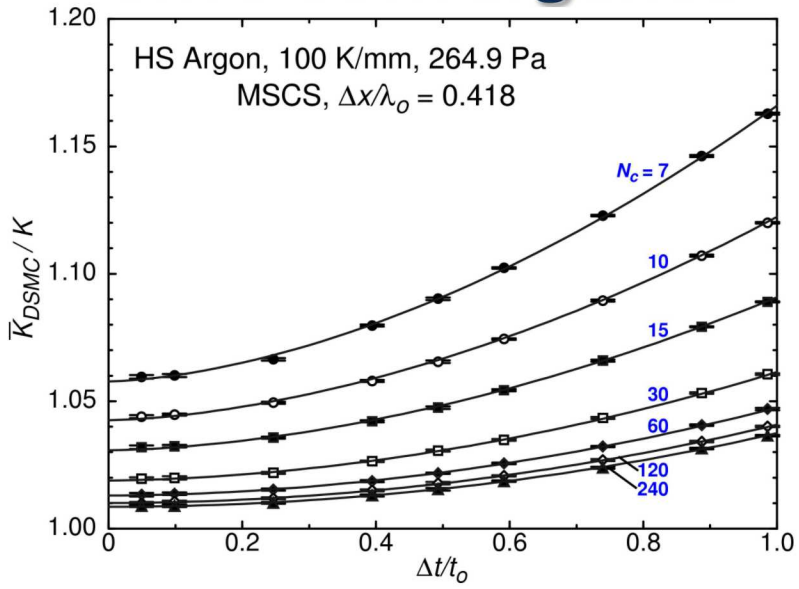

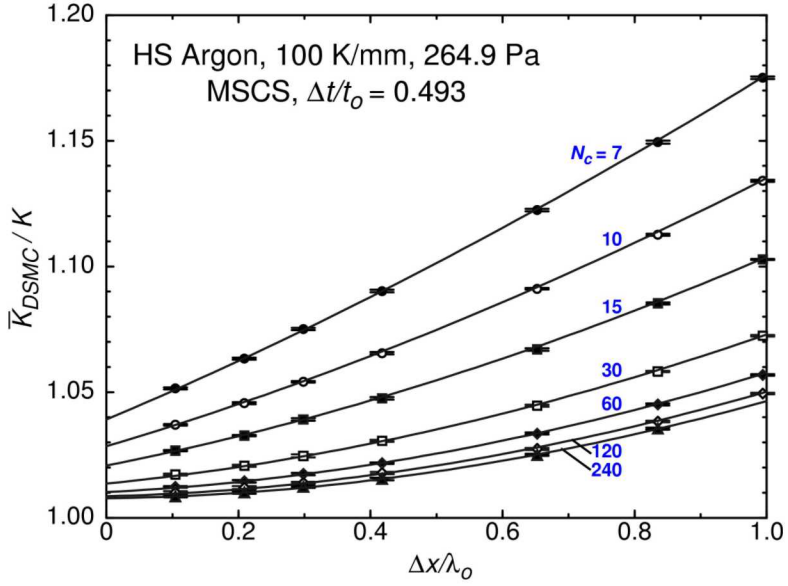

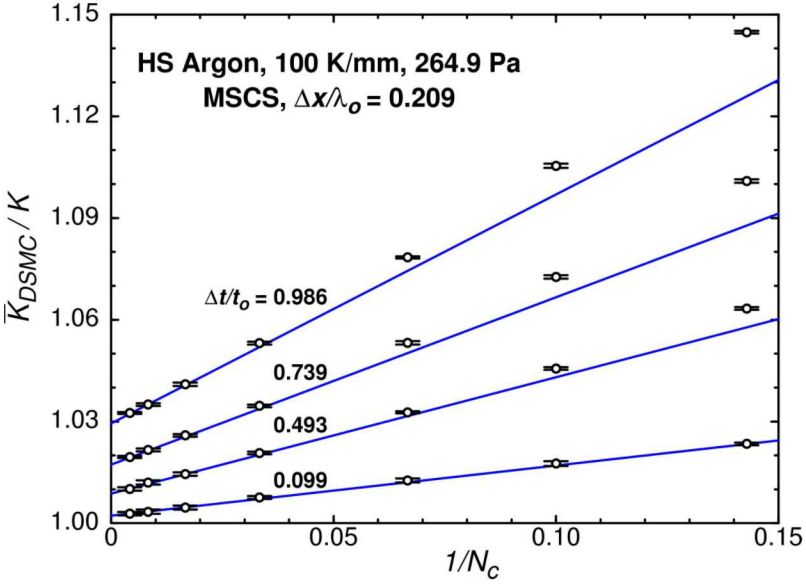

- Curves are best fits
- Error bars represent 95% confidence intervals
- Quadratic convergence for Δx, Δt
- First-order convergence $O(1/N_c)$, as $N_c \to \infty$
- Higher-order for long time steps
- For $N_c = 7$ and $\Delta t/t_o = 0.493$, convergence rate appears linear in $\Delta x/\lambda_o$

Functional Form of Error

Sandia National Laboratories

Functional form that represents DSMC data

- *Ad hoc* series expansion in Dx, Dt, and $1/N_c$
- Perform least-squares fitting of entire data set

$$\frac{K_{DSMC}}{K} = 1.0000 + 0.0286\Delta\tilde{t}^2 + 0.0411\Delta\tilde{x}^2 - 0.0016\Delta\tilde{x}^3 - 0.023\Delta\tilde{t}^2\Delta\tilde{x}^2 +$$
$$-\frac{0.111}{N_c} + \frac{1}{N_c}\left[1.22\Delta\tilde{x} - 0.26\Delta\tilde{x}^2 + 0.97\Delta\tilde{t}^{3/2} + \ldots\right] + 0.95\frac{\Delta\tilde{t}^2}{N_c^2} + \ldots$$

Cross terms show convergence behavior is complex

Rader D. J., Gallis M. A., Torczynski J. R., Wagner W., "DSMC Convergence Behavior of the Hard-Sphere-Gas Thermal Conductivity for Fourier Heat Flow", *Phys. Fluids*, 18, 077102, 2006.

DSMC Numerical Error

Sandia National Laboratories

Traditional DSMC rule-of-thumb guidelines:

- Take enough samples to drive statistical error down to "acceptable" level
- Keep time step smaller than ~1/4 mean collision time
- Keep cell size smaller than ~1/3 mean free path
- Use a minimum of ~20 particles per cell

These guidelines give 2% error, which is similar to the uncertainty in measured transport properties for most gases

- DSMC is subject to the same constraints as other numerical methods.
- DSMC is correct to the limit of vanishing discretization.

Infinite-Particle Convergence

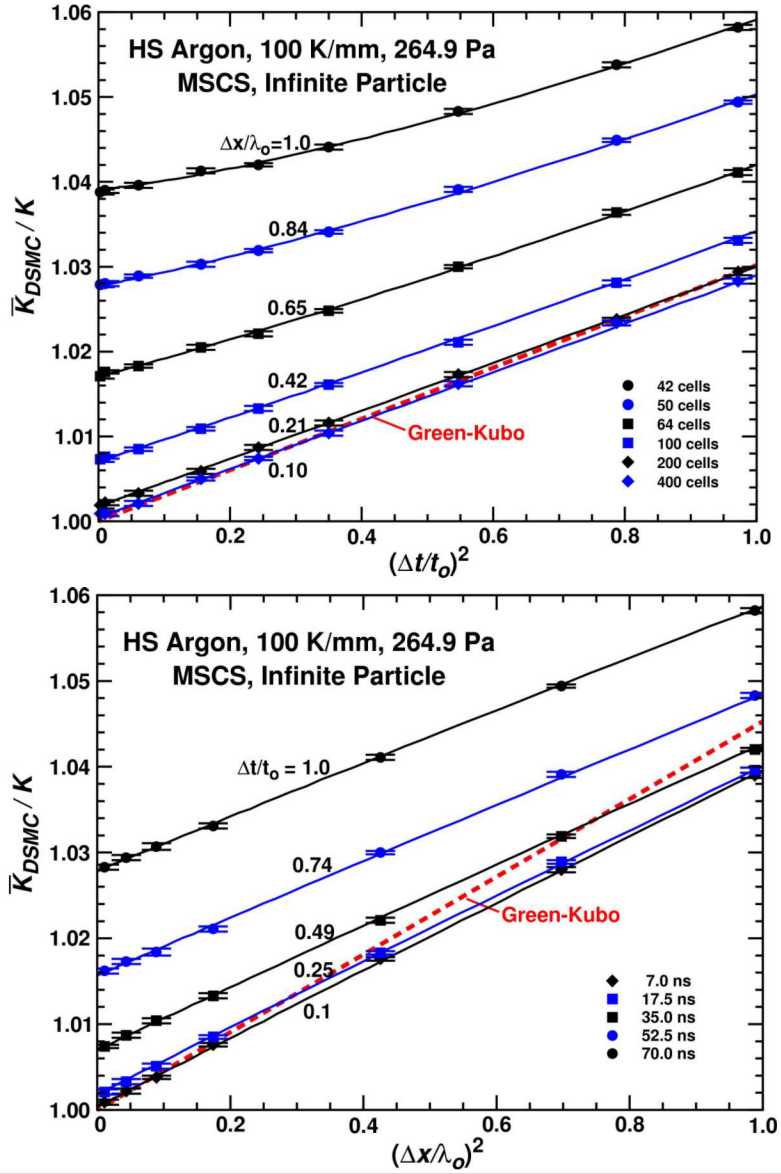

- Finite-particle error removed: values "extrapolated" to $N_c \rightarrow \infty$
- 63 extrapolated data points
- Error bars: fitting uncertainty
- Quadratic convergence in time step and cell size
- *Qualitative* agreement with *Green-Kubo* theory, but slopes are different
- Lines are best fits of data

Could the N-S Equations be extended ?

- Velocity-slip and Temperature jump

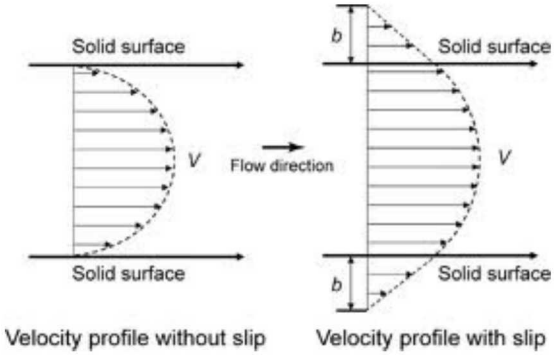

- Modified transport coefficients (viscosity, conductivity, diffusivity)

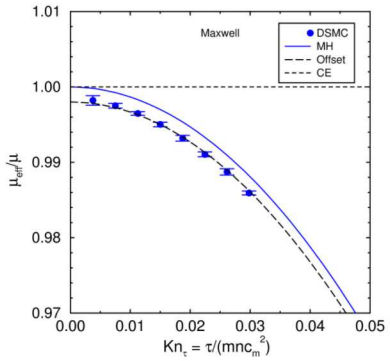

- Hybrid Schemes (NS-DSMC)

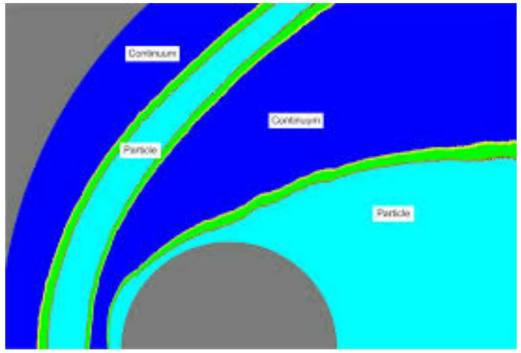

Gas Flow in a Microscale Tube

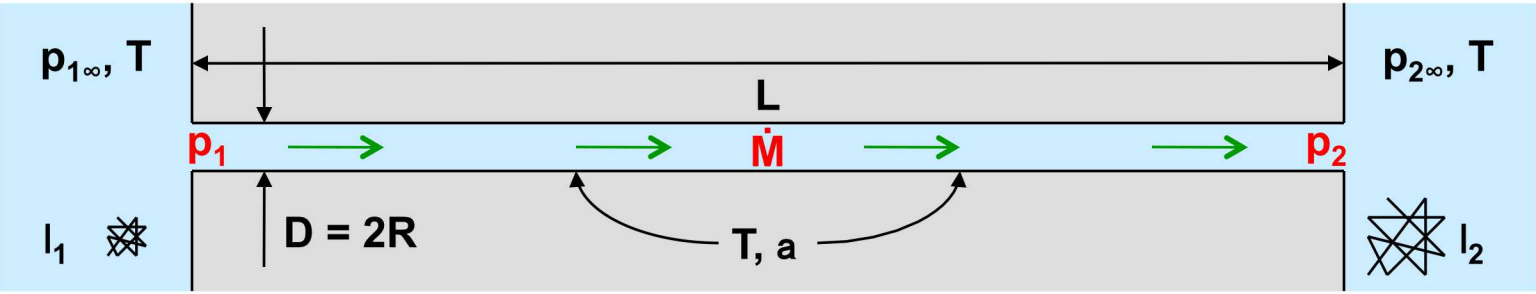

Investigate steady isothermal gas flow in microscale tube

- Tube is long and thin (L >> D) with circular cross section
- Tube joins gas reservoirs at different pressures ($p_{1\infty} \geq p_{2\infty}$)
- Tube and reservoirs have same temperature (T)
- Molecules partially accommodate ($a \leq 1$) when reflecting
- Flow speed << molecule speed, laminar, no turbulence

Determine the mass flow rate and the pressure profile

- General physics-based closed-form expressions
- Free-molecular to continuum (arbitrary mean free path l)
- Theory and molecular-gas-dynamics simulations

Extending the Navier-Stokes equations

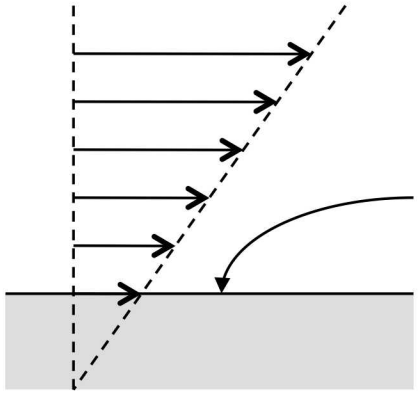

slip velocity

$$U_S - U_W = \frac{2-\alpha}{\alpha}\left\{\frac{\mathrm{Kn}}{1-b\mathrm{Kn}}\left(\frac{\partial U}{\partial n}\right)_s\right\}$$

- Mean free path at STP is 0.06 mm, large enough to matter
- Silicon channels of <10 μm height and >10 μm length

- Accurate mass flow rate needs accurate velocity profile
- Slip boundary condition improves prediction by Navier-Stokes equations

Boundary Conditions for Accurate Transport

Sandia National Laboratories

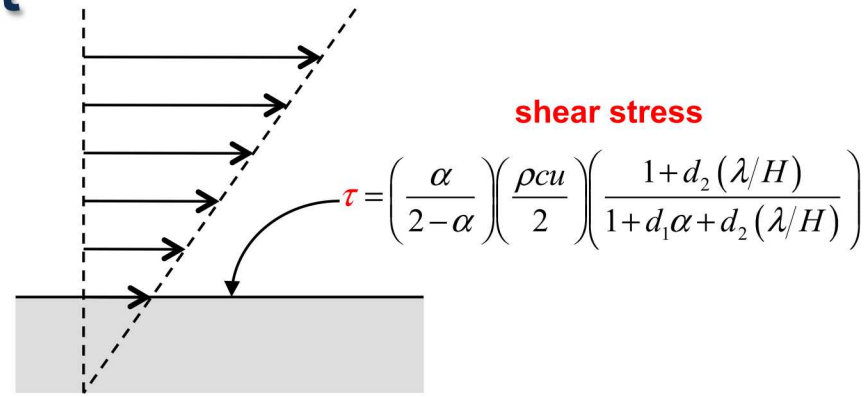

- Transport rates are of primary importance
  - Mass, momentum, energy
- Fields are of secondary importance
  - Concentration, velocity, temperature

Construct boundary conditions to give accurate transport

- When used with Navier-Stokes equations
- For free-molecular, transition, slip, continuum

Resulting fields are only qualitatively correct

- Fields are accurate in continuum limit

Mass Flow Rate Has Correct Limits

Sandia National Laboratories

Approximate Closed-Form Expression

$$\dot{M} = \dot{M}_C\left(1+\frac{8p_\lambda}{p_m}\varpi\left[p_1,p_2\right]\right),\quad \varpi\left[p_A,p_B\right]=\frac{2-\alpha}{\alpha}\left\{1+b_1\alpha+\left(\varepsilon b_0-1-b_1\alpha\right)\frac{b_2p_\lambda}{p_A-p_B}\ln\left[\frac{p_A+b_2p_\lambda}{p_B+b_2p_\lambda}\right]\right\}$$

Continuum

$$\dot{M}_C=\frac{D^4p_m\left(p_1-p_2\right)}{16\mu c^2L}$$

Slip

$$\dot{M}_S=\dot{M}_C\left(1+\frac{8p_\lambda}{p_m}\varpi_S\right),\quad \varpi_S=\frac{2-\alpha}{\alpha}\left(1+b_1\alpha\right)$$

Free-Molecular

$$\dot{M}_F=\dot{M}_C\left(\frac{8p_\lambda}{p_m}\varpi_F\right),\quad \varpi_F=\frac{2-\alpha}{\alpha}\varepsilon b_0$$

Continuum Orifice

$$\dot{M}_{OC}=\frac{R^3\rho_{m\infty}}{3\mu}\left(p_{1\infty}-p_{2\infty}\right)$$

Free-Molecular Orifice

$$\dot{M}_{OF}=\pi R^2\frac{mc}{4}\left(n_{1\infty}-n_{2\infty}\right)$$

Free-Molecular Short Tube

$$\dot{M}_{TF}=\dot{M}_{OF}\Big/\left(1+\left(\alpha L/D\right)\right),\quad \alpha L/D\ll 1$$

Expression reproduces known limits correctly

Continuum	Not affected by ε, b_0, b_1, b_2
Slip	Determined by b_1
Free-Molecular	Determined by ε, b_0
Orifice/Short-Tube	Determined by ε, b_0

Ewart et al. (2006) Tube Experiments

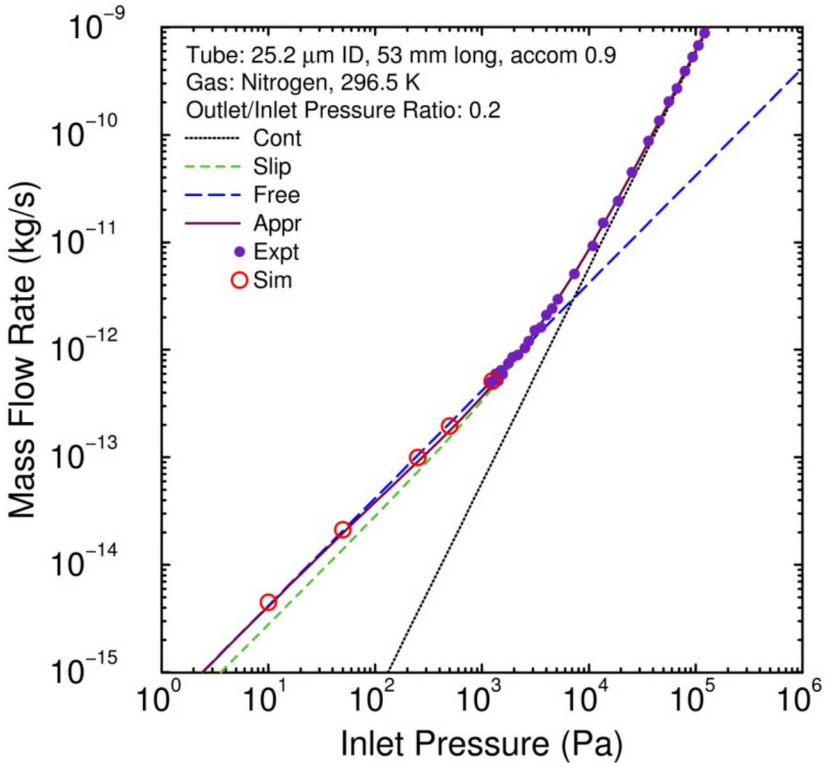

Tube Mass Flow Rate

$$\dot{M} = \dot{M}_C\left(1+\frac{8p_\lambda}{p_m}\varpi\left[p_1,p_2\right]\right),\quad \dot{M}_C = \frac{D^4}{16}\frac{p_m\left(p_1-p_2\right)}{\mu c^2 L}$$

$$\varpi\left[p_A,p_B\right] = \frac{2-\alpha}{\alpha}\left\{1+b_1\alpha+\left(\varepsilon b_0-1-b_1\alpha\right)\frac{b_2p_\lambda}{p_A-p_B}\ln\left[\frac{p_A+b_2p_\lambda}{p_B+b_2p_\lambda}\right]\right\}$$

$$\rho = \frac{mp}{k_BT},\ \mu=\mu[T],\ c=\sqrt{\frac{8k_BT}{\pi m}},\ \lambda=\frac{2\mu}{\rho c},\ p_\lambda=\frac{p\lambda}{D},\ p_m=\frac{p_1+p_2}{2},\ \mathrm{Kn}_m=\frac{p_\lambda}{p_m}$$

$$\frac{\alpha L}{D}>10^3,\ \varepsilon\to 1,\ p_1\to p_{1\infty},\ p_2\to p_{2\infty};\ b_0=\frac{16}{3\pi},\ b_1=0.15,\ b_2=\frac{0.7\alpha}{2-\alpha}$$

Same values of e, b_0, b_1, b_2 used for all circular tubes
Values are unchanged from previous cases (no adjusting)
Relative to diameter, this tube length is essentially infinite

Mass flow rate measured for silica microscale tube

- D = 25.2 mm, L = 53 mm, a = 0.9, N_2, T = 296.5 K, p_2/p_1 = 0.2

Expression and simulations agree well with experiment

- Lowest experiment pressure is above Knudsen minimum
- Highest simulation pressure reaches experiment

IPL and VSS Molecules

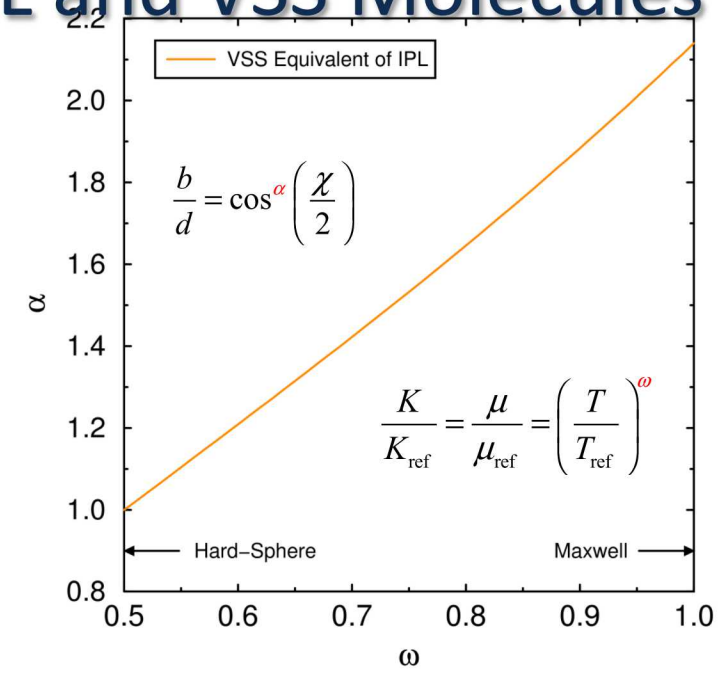

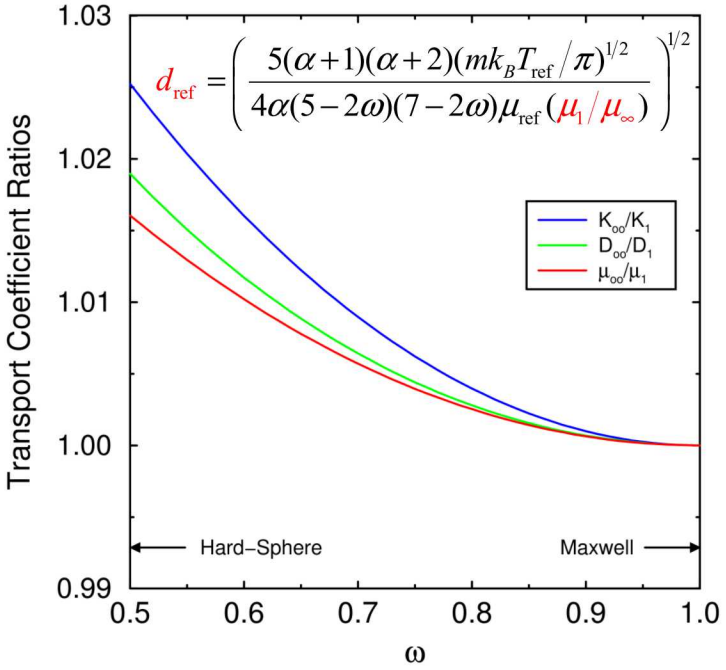

Best VSS *w*, *a* to match IPL *w* by equating diffusivities

- Identical match only for hard-sphere
- VSS-Maxwell ≠ IPL-Maxwell (they are very similar)

Infinite-approximation CE changes K and m by $O(0.03)$

- Affects reference diameter d_{ref} very slightly

Transport Coefficients

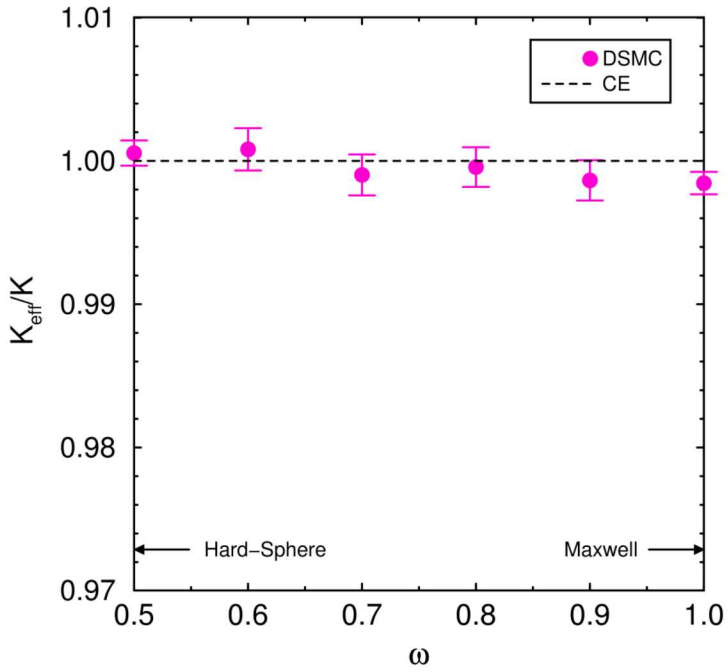

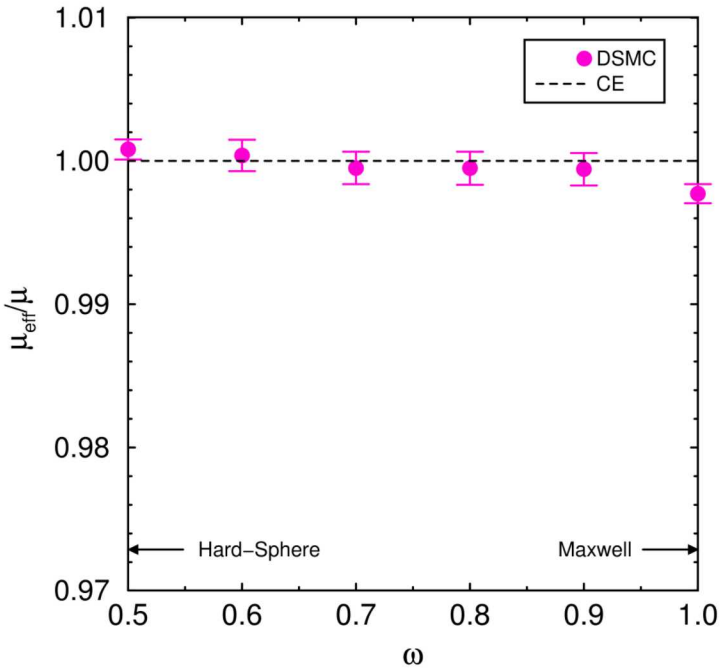

Thermal conductivity and viscosity for IPL molecules

- Intermolecular force: hard-sphere through Maxwell
- Stochastic and discretization errors: ± 0.002 each
- CE infinite-to-first-approximation difference: $O(0.03)$

Excellent agreement between DSMC and CE

Sonine Coefficients

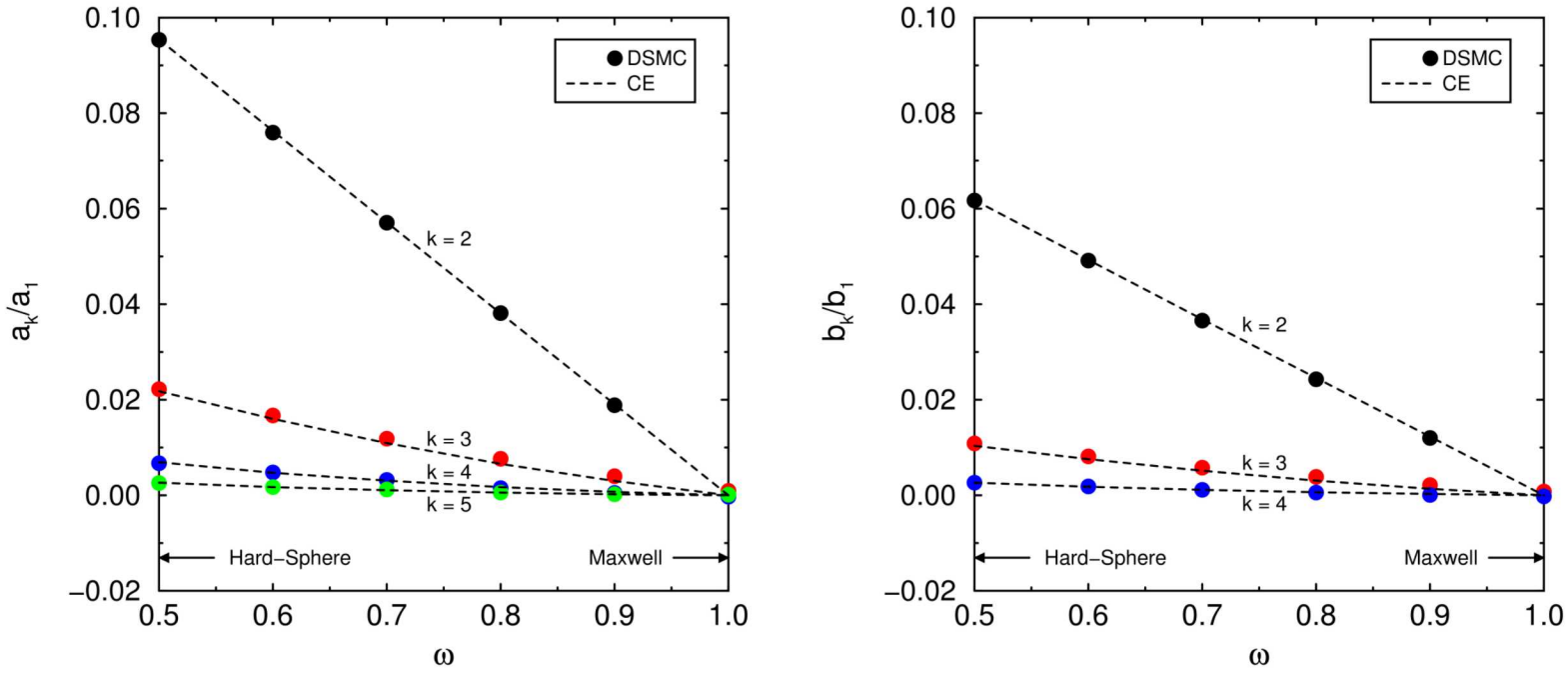

Sonine coefficients a_k/a_1 and b_k/b_1 for IPL molecules

- Intermolecular force: hard-sphere through Maxwell
- Stochastic, discretization errors: smaller than symbols

Good agreement between DSMC and CE

- Higher-k coefficients have similar agreement
- Slight difference for $k = 3$, Kn_q not small enough

Hard-Sphere Sonine Coefficients

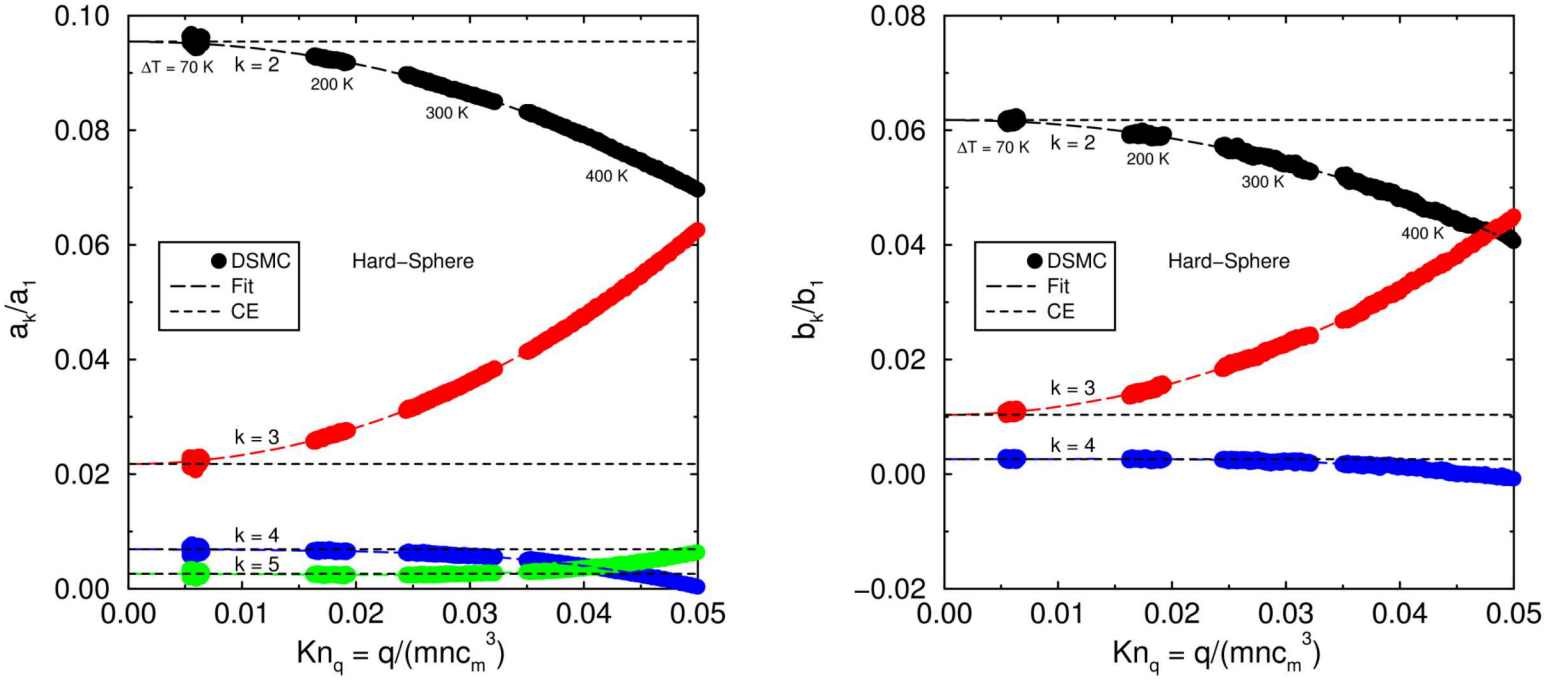

Hard-sphere normal solutions for a_k/a_1 and b_k/b_1

DSMC hard-sphere and VSS-Maxwell have same trends

- Four DSMC simulations at same conditions as Maxwell
- No exact results available: MH does not apply
- Even-k terms decrease, odd-k terms increase

Hard-Sphere Normal Transport Coefficients

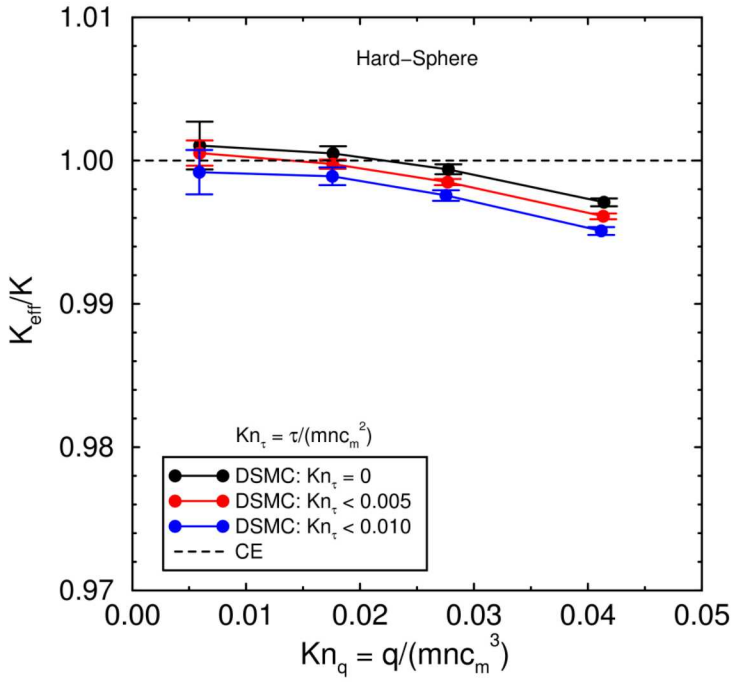

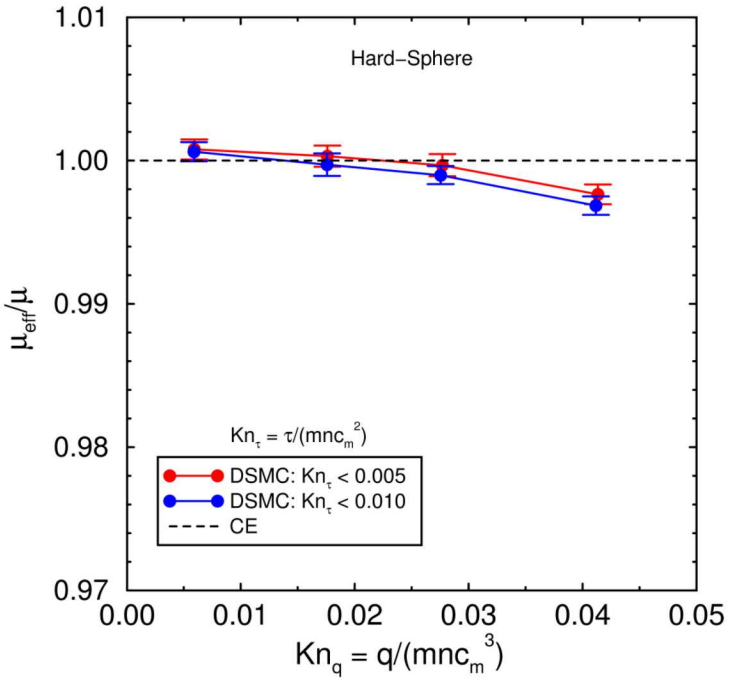

DSMC hard-sphere normal solution for K and m

- No theoretical results available: MH does not apply
- DSMC values decrease slightly with Kn_q
- Difference apparently greater than discretization error

Hard-sphere gas: “flux-insulating” and “flux-thinning”

Hard-Sphere Normal Transport Coefficients

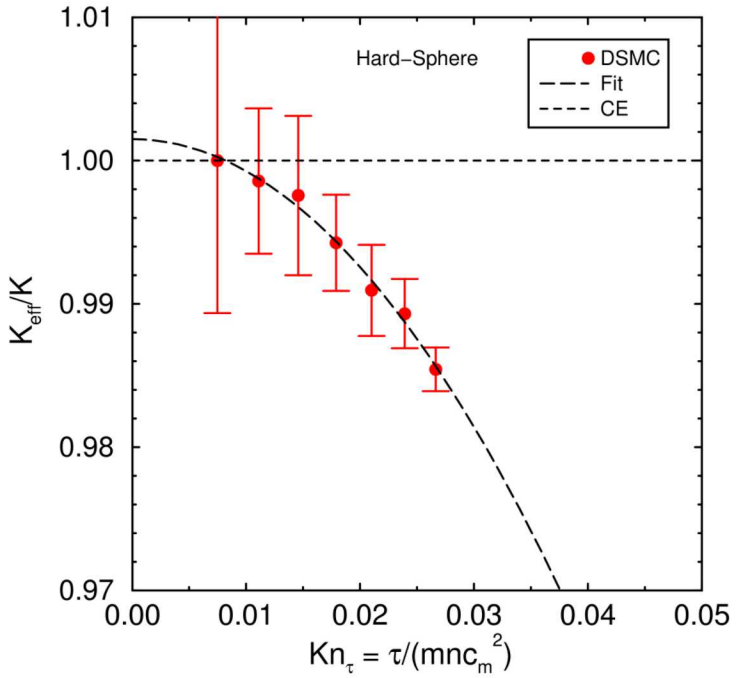

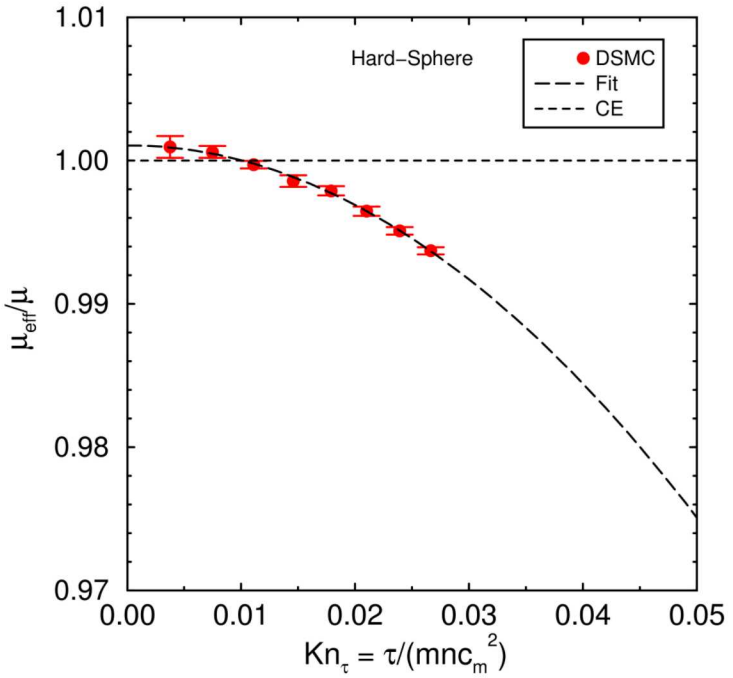

DSMC hard-sphere normal solution for K and m

- Finite Kn_t (shear stress), low Kn_q (heat flux)
- No theoretical results available: MH does not apply
- DSMC values decrease with Kn_t (like Maxwell)

Hard-sphere gas: “shear-insulating” and “shear-thinning”

Maxwell Sonine-Coefficient Profiles

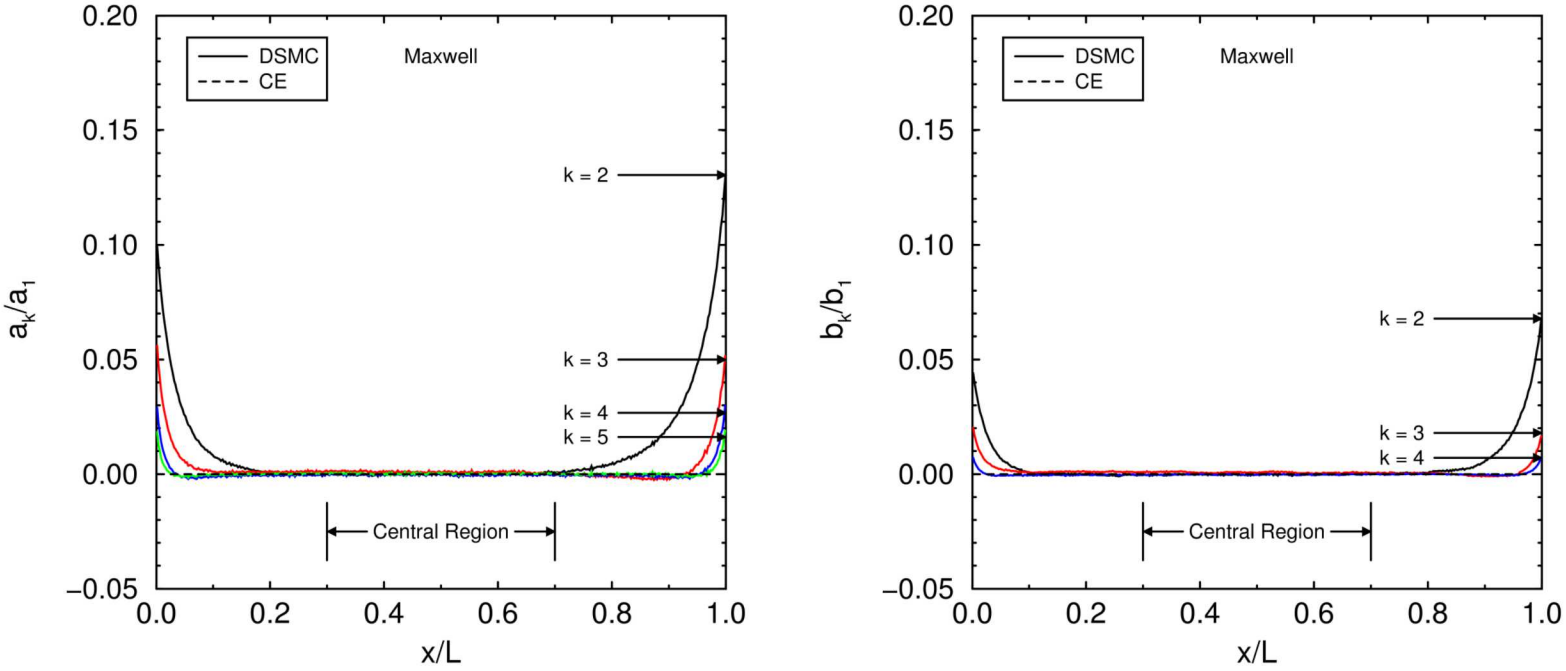

DSMC and CE Maxwell coefficients a_k/a_1 and b_k/b_1

- Low heat flux, low shear stress: $Kn_q = 0.006$, $Kn_\tau = 0.003$
- Good agreement in central region: normal solution
- Knudsen layers easily observed: ~10% of domain

Continuum but Non-equilibrium in MEMS Heated Microbeam Near Substrate

Sandia National Laboratories

Non-equilibrium may be observed in continuum conditions

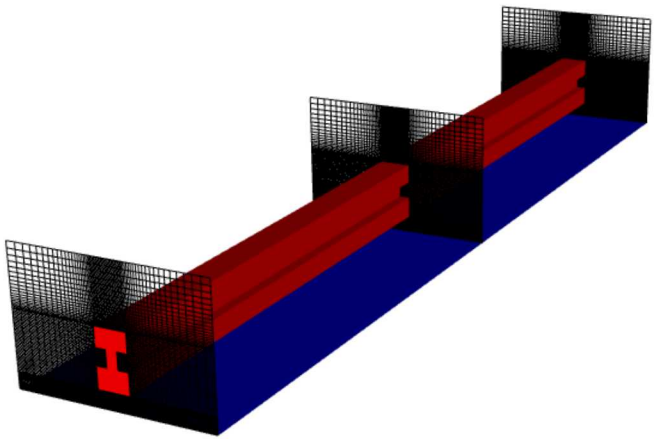

Solid regions: silicon

- Geometry: 2-micron gap
- Beam temperature: ~900 K
- Substrate temperature: ~300 K

Gas region: nitrogen

- Pressure: atmospheric
- Initial temperature: ~300 K
- **Mean free path: 70 nm**

Heated Microbeam Makes Gas Move

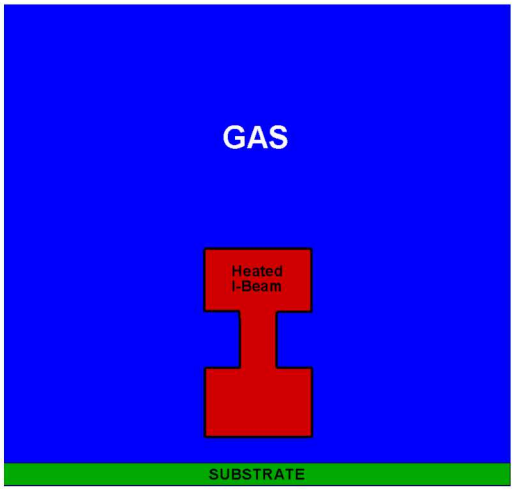

DSMC microbeam simulations

- Steady gas motion is induced by temperature differences

  Not buoyancy, *not* transient
- Noncontinuum effects cause motion

  Not seen in NSSJ simulations

1 atm
~0.1 m/s

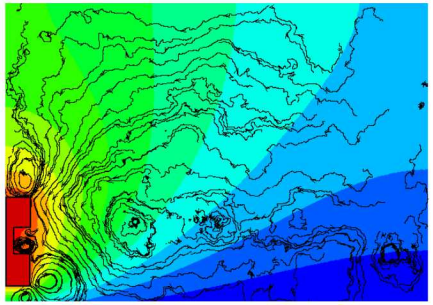

0.1 atm
~2 m/s

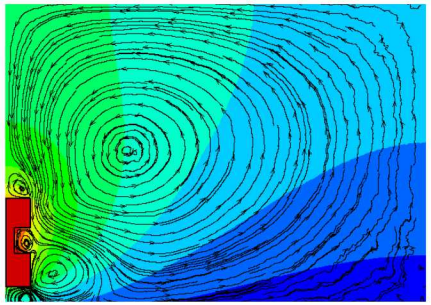

0.01 atm
~1 m/s

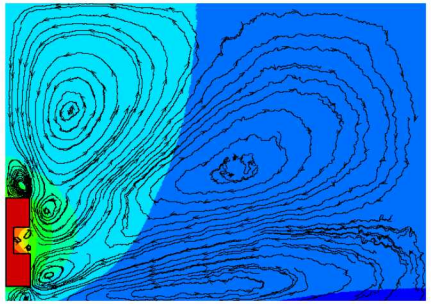

Maxwell Normal Transport Coefficients

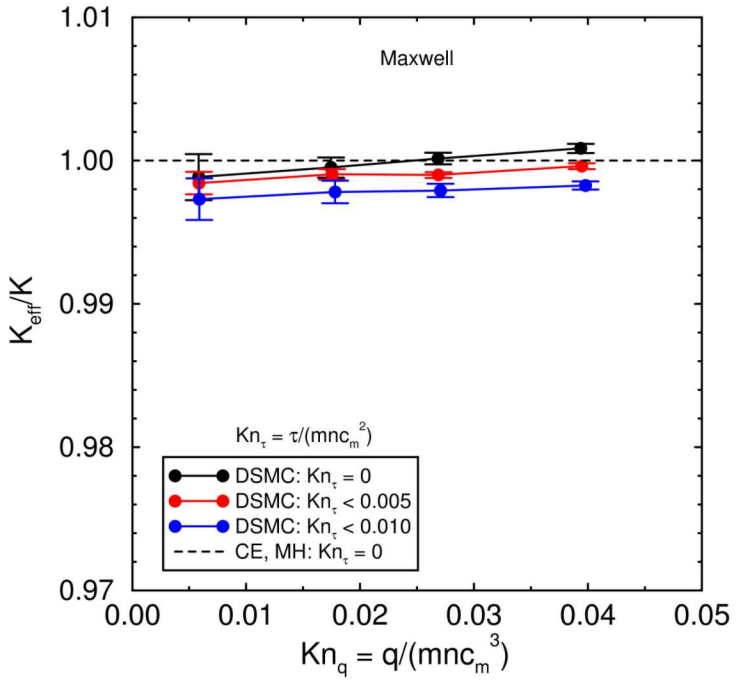

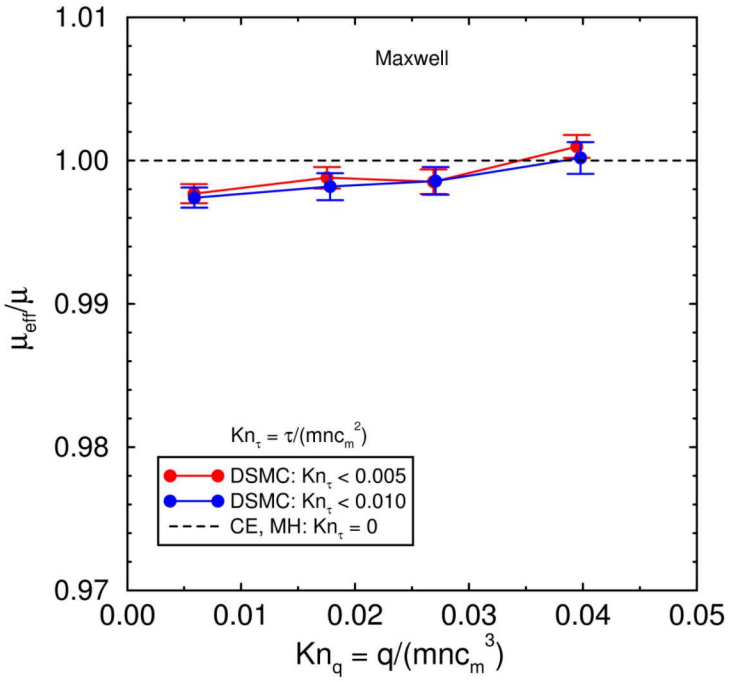

DSMC and MH Maxwell normal solutions for K and μ

- DSMC profiles look like low-Kn_q profiles
- MH values for $Kn_\tau = 0$ are independent of Kn_q
- DSMC values approach MH values as $Kn_\tau \rightarrow 0$
- DSMC values increase very slightly with Kn_q

Agree to within DSMC discretization error

Rarefied Gas Dynamics Regime

- High Mach number flight is more easily achieved in rarefied conditions (low-density, low-friction)
- When low-density/non-continuum conditions prevail, flows are out of thermodynamic equilibrium
  - Not enough molecular collisions to maintain LTE
- This flight regime results in high temperatures (more than 10,000 K), chemically reacting, ionizing, radiating flows

  pushing the flow further away from equilibrium
- In the rarefied, hypersonic regime the NS equations are usually not applicable

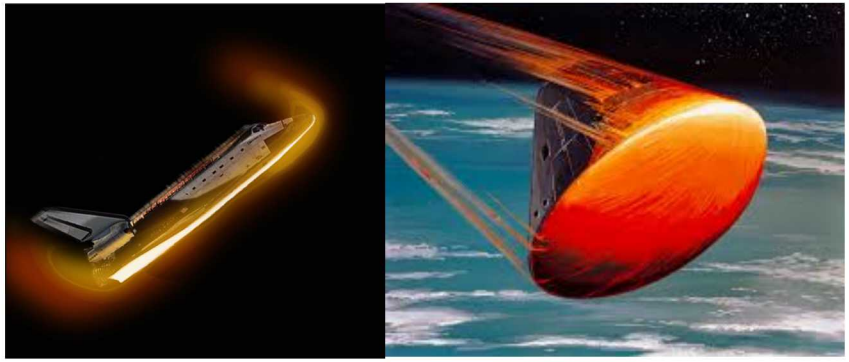

Diffusing energy through re-entry

Sandia National Laboratories

Gemini 1961-1966	Apollo 1963-1972	Space Shuttle 1981-2011	Orion 2014-?
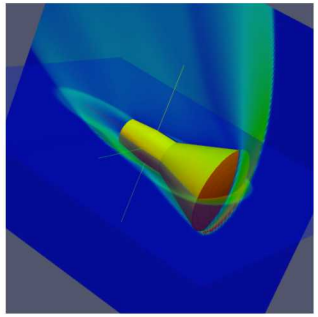	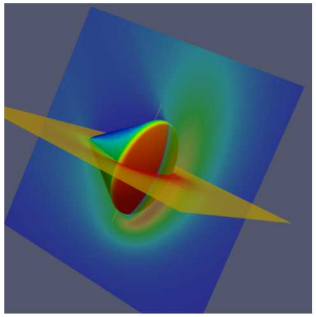	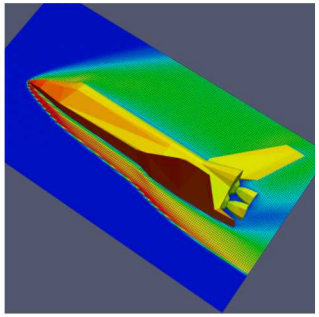	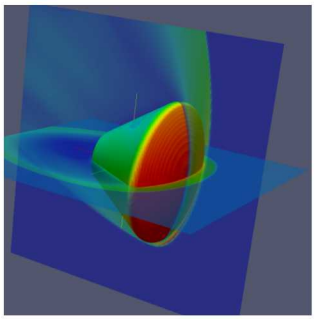
			

- Atmospheric entry system must provide controlled dissipation of kinetic and potential energy of the vehicle.
- Dynamic and thermal loads must be kept with certain range

Maxwell Sonine-Coefficient Profiles

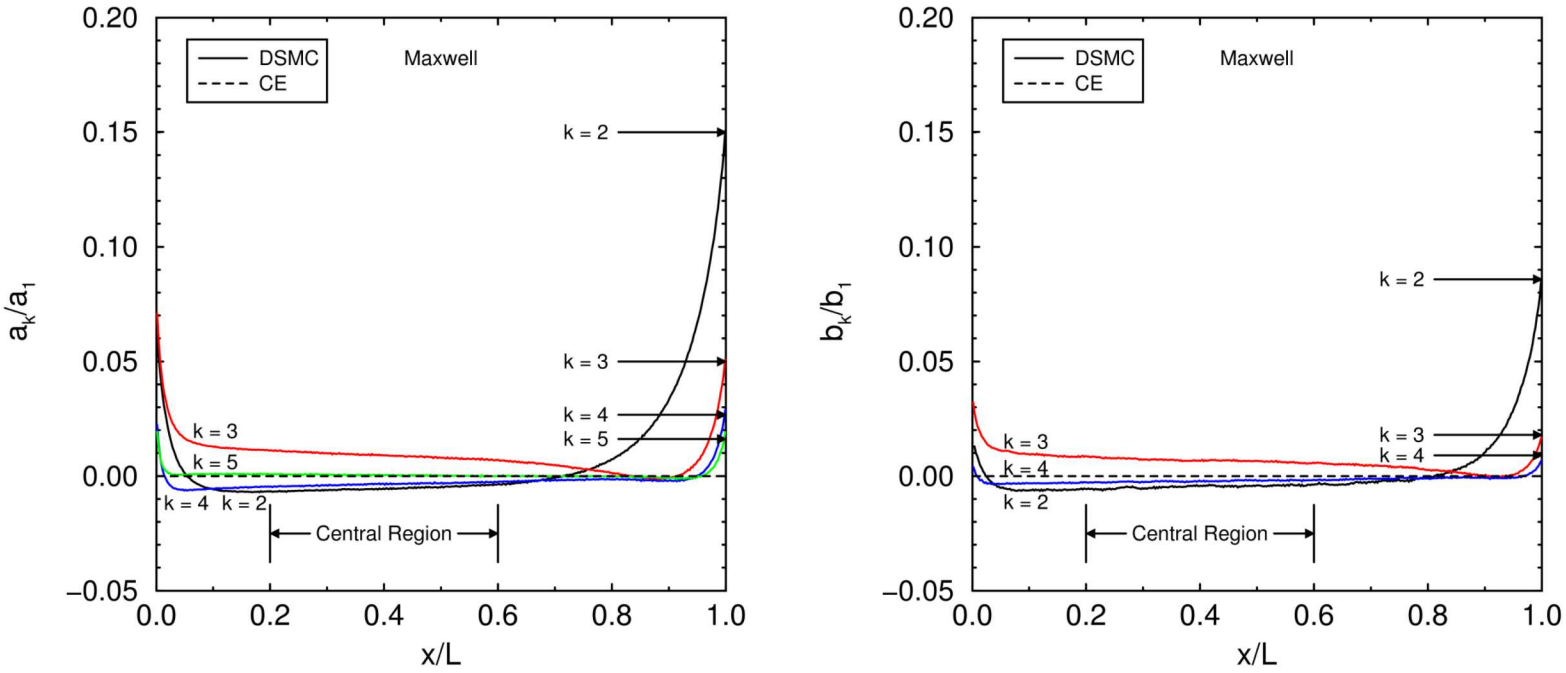

Finite heat flux, low shear stress: $\mathrm{Kn}_q \sim 0.017$, $\mathrm{Kn}_\tau = 0.003$

Maxwell Sonine-polynomial coefficients a_k/a_1, b_k/b_1

- CE and DSMC differ in central region: Kn_q not small
- Normal solution is non-uniform: $\mathrm{Kn}_q \sim T^{-1/2}$ and $T = T[x]$

Plot DSMC values vs. Kn_q from central region

Adaptive Gridding

Sandia National Laboratories

- Create/adapt grid in situ, rather than pre-process & read in
- Examples: Generate around surface to user-specified resolution, adapt grid based on flow properties
- Algorithms should be efficient if they require only local communications

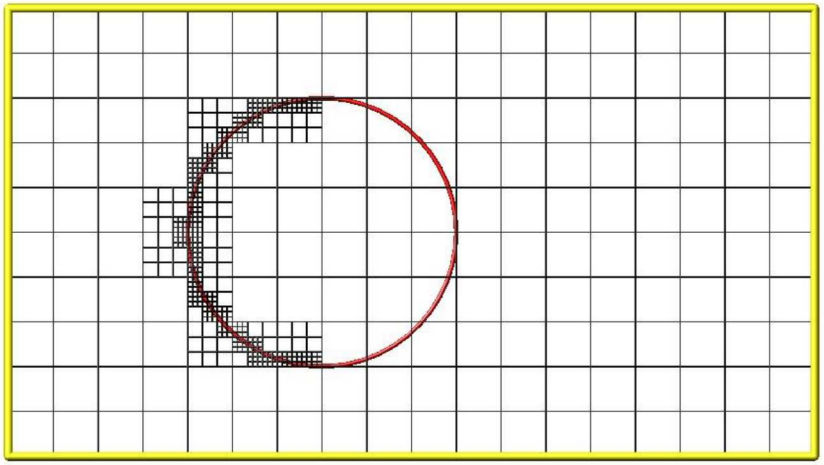

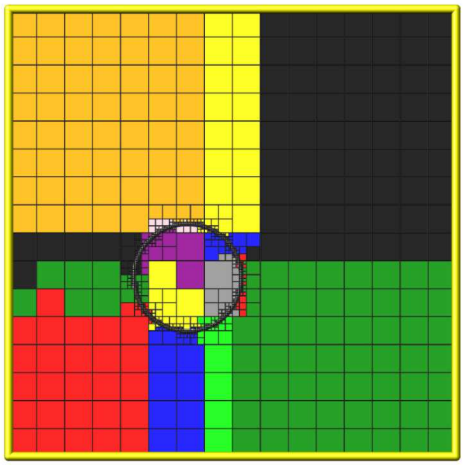

- Another setup task: label cells as outside/inside
- Simple if pre-processing, in situ easier for large problems

SPARTA Benchmarking (FM)

16 cores/node, 1 task/core

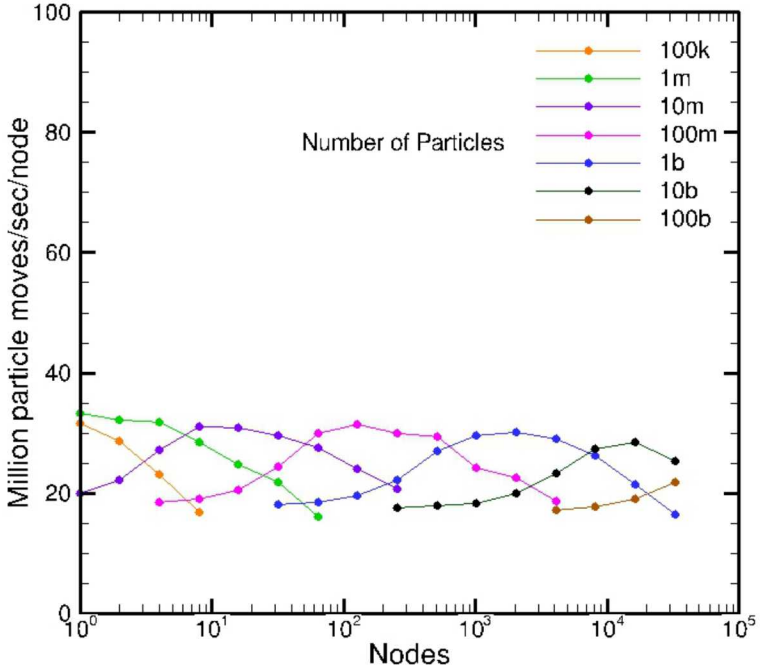

16 cores/node, 4 tasks/core

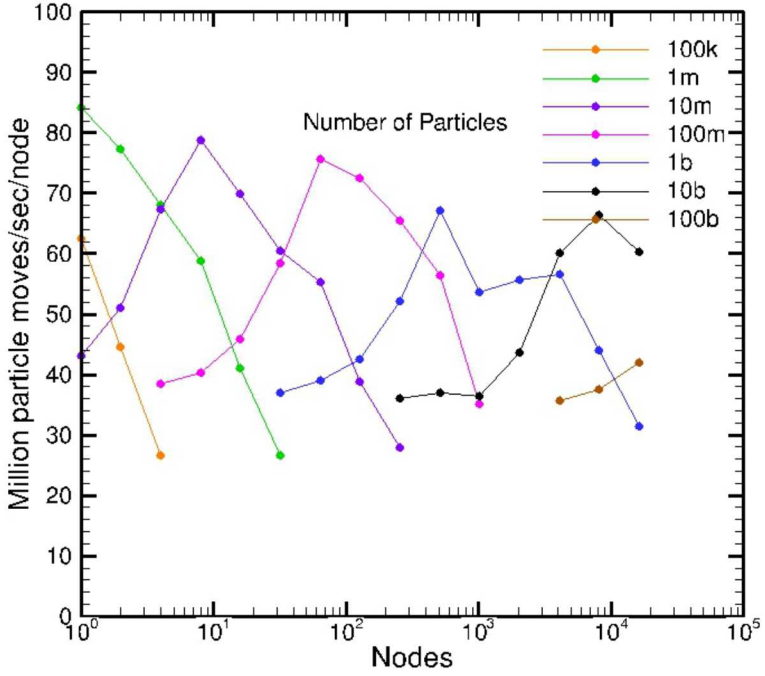

- Free-molecular (FM) calculations stress-test for communications
- 2x speedup compared to collisional

Aiming for MPI+X via Kokkos

Sandia National Laboratories

- What is Kokkos:
  - Programming model in development at Sandia
  - C++ template library
  - Open-source
  - Stand-alone
- Goal: write application kernels only once, and run them efficiently on a wide variety of hardware platforms
- Two major components:
  - Data access abstraction via Kokkos arrays optimal layout & access pattern for each device: GPU, Xeon Phi, etc.
  - Parallel dispatch of small chunks of work auto-mapped onto back-end languages: CUDA, OpenMP, etc.

Torricelli's Mercury Barometer

Evangelista Torricelli

In 1643 Torricelli invented the barometer

The mercury column stands at 0.76 m indicating that atmospheric pressure can support 10 m (=14x0.76 m) of water